SEP 4 19

THE JOURNAL OF CHEMICAL PHYSICS

VOLUME 14 NUMBER 8

AUGUST, 1946

Published by the

AMERICAN INSTITUTE OF PHYSICS

Lancaster, Pa. and New York, N. Y.

THE JOURNAL OF CHEMICAL PHYSICS

BOARD OF EDITORS

Joseph E. Mayer, Editor

Associate Editors

Term ending December 31, 1947	*Term ending December 31, 1948*
Paul C. Cross	Charles D. Coryell
Raymond M. Fuoss	F. O. Rice
John G. Kirkwood	L. H. Thomas
H. Mark	G. W. Wheland
O. Oldenberg	E. Bright Wilson, Jr.
Oscar K. Rice	

THE JOURNAL OF CHEMICAL PHYSICS is published monthly by the American Institute of Physics. Its purpose is to bridge a gap between journals of physics and journals of chemistry. The artificial boundary between physics and chemistry has now been in actual fact completely obliterated, and a large and active group is engaged in research which lies much the one as the other. It is to this group that the Journal is rendering its principal service and making its greatest appeal, both as a prompt and efficient medium for publication of research and as a convenient and carefully edited assemblage of pertinent information.

Notes for Contributors

Manuscripts for publication should be submitted to Joseph E. Mayer, Kent Chemical Laboratory, University of Chicago, Chicago 37, Illinois. Papers are published in English only. To be acceptable for publication manuscript should be original typewritten copy (not carbon copy) either double or triple spaced, with wide margins. References should appear as footnotes only and should be numbered consecutively to avoid repetition. References should include author's name, journal, volume number, page number, and year and should be listed in the order given here. Definition should be given to subscriptions for tables and legends for figures. These in all cases should be complete in themselves so as to make the data intelligible to the reader without consulting the text of the article.

Special care should be given to the mathematical expressions. The very simplest formulas only should be typewritten and all others carefully written in with pen and ink. Fractional exponents should be used to avoid root signs everywhere. Special symbols should be used to avoid complicated exponents. The solidus (/) should be used wherever possible for fractions.

All illustrations should accompany manuscript and should always be referred to in the text. Line drawings must be made with India ink on plain white paper or on tracing cloth. Coordinate paper is not desirable, but if used must be blue-lined with all coordinates to be reproduced drawn with India ink. Lettering should be of sufficient size to be legible after reduction.

Proof and all correspondence concerning papers in the process of publication should be addressed to the Publications Manager, American Institute of Physics, 57 East 55 Street, New York 22, New York.

Subscription Price

The United States and Possessions, Canada and Mexico $10.00
Elsewhere 11.00

Back Numbers

Complete set: Vol. 1, 1933—Vol. 13, 1945 ..... $130.00
Yearly rate: $11.00.
Single copies: $1.00 each.

Subscriptions and orders for single copies should be addressed to Prince and Lemon Streets, Lancaster, Pennsylvania, or to the American Institute of Physics, 57 East 55 Street, New York 22, New York.

Changes of address should be sent to the Business Manager, American Institute of Physics.

The Journal of Chemical Physics is published monthly at Prince and Lemon Streets, Lancaster, Pennsylvania.

Entered as second class matter December 20, 1932, at the Post Office at Lancaster, Pa., under the Act of August 24, 1912. Acceptance for mailing at special rate of postage, provided for in the Act of February 28, 1925, embodied in paragraph 4, Section 538, P. L. & R.: authorized [illegible]

THE JOURNAL
OF
CHEMICAL PHYSICS

VOLUME 14, NUMBER 8 AUGUST, 1946

The Photochemical Polymerization of Butadiene[1]

DAVID H. VOLMAN
Noyes Chemical Laboratory, University of Illinois
and
Division of Chemistry, College of Agriculture, University of California, Davis, California

(Received May 10, 1946)

The mercury photo-sensitized polymerization of butadiene and butadiene-acetone mixtures in the gas phase, and the photochemical reactions in solutions of butadiene and acetone in hexane, were studied. Metal mirror experiments demonstrated the absence of hydrogen atoms and the presence of alkyl radicals at low pressures. The mechanism proposed for butadiene vapor postulates an activated butadiene molecule produced by collision with activated mercury and competition between deactivation by collision, predissociation into free radicals, and a collisional process to give hydrogen gas. The polymerization chain proceeds by a mechanism involving either free radicals or hydrogen atoms. In the presence of acetone vapor, the rate is increased and the increase is directly proportional to the number of free radicals coming from acetone, indicating that polymerization chains are not broken by bimolecular gas phase reaction between free radicals. The quantum yield for butadiene alone at 53-mm pressure and 43°C was 0.24. The average number of molecules reacting per free radical formed was calculated to be between 3 and 8. The liquid solution results are explained on the basis of a modified Frank-Rabinowitch hypothesis for the primary photochemical process. Activated acetone molecules are deactivated by collision with hexane, and react with acetone to yield unsaturated compounds and with butadiene to initiate polymerization. The following kinetic equation is developed for the rate of polymerization, $dP/dt=(kI_{abs}/I_0)(n[C_4H_6]-[(CH_3)_2CO])$, where n is the average number of molecules reacting per free radical. n is taken equal to 4.

INTRODUCTION

THE polymerization of alkadienes in the presence of free radicals in the liquid phase is a well-known reaction leading to the production of polymers. Since photochemical methods may be used to introduce free radicals into a system, it was thought that it would be of interest to investigate the polymerization of butadiene induced by free radicals obtained from decomposing acetone in ultraviolet light. The fact that butadiene is transparent at wave-lengths greater than 2300A[2] and that aliphatic ketones absorb light and yield free radicals in the wave-length region greater than 2300A[3] permits such an experiment.

In general photochemical reactions in the liquid state are complicated in comparison to reactions in the gas state because of solvent effects. Therefore it was considered valuable to study the vapor phase reaction involving butadiene as a preliminary to work in liquid solutions.

[1] The experimental work reported herein was carried out at the University of Illinois under the sponsorship of the Office of Rubber Reserve, Reconstruction Finance Corporation, in connection with the Government's synthetic rubber program.

[2] G. Scheibe and H. Grieneisen, Zeits. f. physik. Chemie **B25**, 52 (1934).

[3] R. G. W. Norrish, Trans. Faraday Soc. **33**, 1521 (1937).

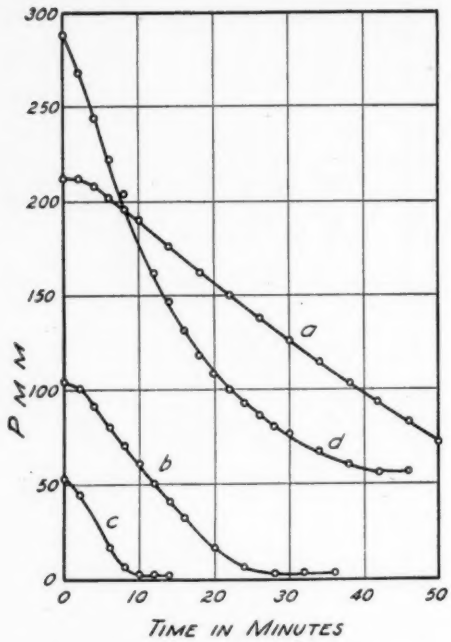

FIG. 1. Pressure *vs.* time for some typical experiments. *a*, *b*, and *c* are for butadiene alone. *d* is for 106-mm acetone and 182-mm butadiene initially present.

PART I. THE MERCURY SENSITIZED VAPOR PHASE REACTION OF BUTADIENE AND BUTADIENE-ACETONE MIXTURES

Gee[4] and later Gunning and Steacie[5] have carried out investigations on the mercury photosensitized polymerization and hydrogenation of butadiene. Gunning and Steacie were apparently unaware of the earlier work, and their paper contains no evaluation of the findings of Gee. In the present study some further experiments on the mercury sensitized reaction of butadiene are reported. In addition, experiments on the mercury sensitized reaction of butadiene-acetone mixture were carried out.

Experimental

Glass tubes containing butadiene and acetone were attached to the irradiation system by ground glass joints and stopcocks. No precautions to eliminate the use of stopcock grease were taken since, with the intense lamp used, the rates of reaction were great enough so that the absorption of butadiene by lubricant was negligible. The reaction tube was a quartz cylinder, 30 mm ×200 mm, ending in Pyrex seals at either end. Provision for evacuating the system by a mercury diffusion pump was made. The remainder of the apparatus consisted of suitable traps, a McLeod gauge, and a mercury manometer for following the pressure changes. In practice some liquid mercury was always placed inside the reaction tube in order to insure constant mercury vapor pressure.

At the start of an experiment, previously outgassed butadiene or acetone was allowed to enter the outgassed reaction tube until the proper pressure was established. The vapors were then frozen out with liquid air and any residual uncondensed gas was pumped off. The mercury resonance lamp, in the shape of a helix around the reaction tube, was allowed to warm up for fifteen minutes, sufficient time for the lamp to become constant and thermal equilibrium to be established. The light shields were then removed and the pressure of the system followed by the manometer. The temperature of the system was 43±1°C.

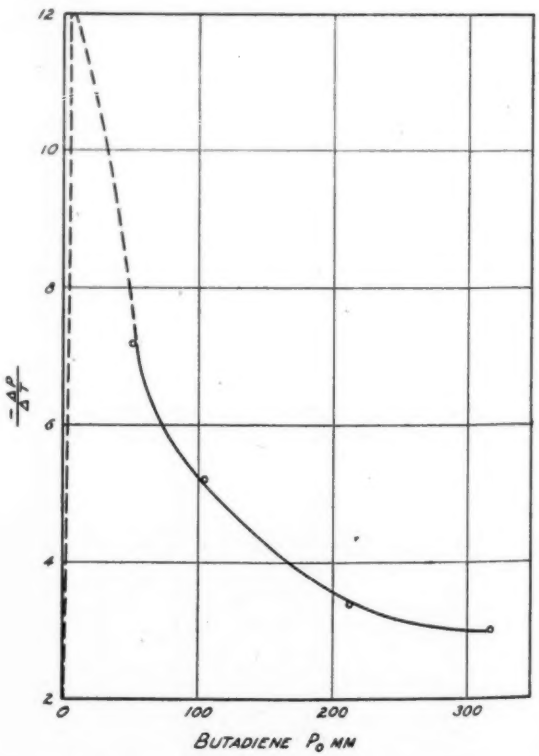

FIG. 2. The initial rate *vs.* the initial butadiene pressure in the absence of acetone.

[4] G. Gee, Trans. Faraday Soc. **34**, 712 (1938).
[5] H. E. Gunning and E. W. R. Steacie, J. Chem. Phys. **12**, 484 (1944).

The light source was of the rare gas mercury vapor type supplied by the Hanovia Company, which emits most of its radiation as the mercury resonance wave-length, 2537A.

Rate of the Reaction

The rate of the reaction at various butadiene pressures in the absence of acetone, and the rate of the reaction for various acetone pressures and a fixed butadiene pressure, were followed. Figure 1 shows typical curves obtained when total pressure in the system is plotted against time of illumination for experiments carried out at 43°C. It may be seen that for butadiene alone the reaction starts slowly at the highest pressure and more rapidly at the lower pressures. The rate then reaches a maximum and diminishes slowly until near the end of the reaction when it tapers off rapidly. The experiment represented by curve *a* was carried to completion, but only the first 50 minutes are shown. The course of the reaction was not substantially different from the experiments represented by curves *b* and *c*. In each case a few mm of gas uncondensable at liquid-air temperature remains. When acetone is added, curve *d*, the reaction starts out rapidly but slows up gradually and stops while considerable pressure remains.

After a preliminary adjustment period the course of the reaction proceeds smoothly, the maximum rate being reached a few minutes after irradiation begins. In Fig. 2 this initial reaction rate or slope of the *P vs. t* curve, Fig. 1, is plotted as a function of butadiene pressure for experiments in which butadiene was the sole reactant and in Fig. 3 against acetone pressure for experiments in which the initial butadiene pressure was constant and the initial concentration of acetone was varied. The broken portion of Fig. 2 was extrapolated from the data of Gunning and Steacie[5] since they covered the pressure region below 50 mm while the present work was carried out at higher pressures. In the extrapolation allowance was made for the differences in intensity of illumination used.

The Quantum Yield

Since the absorption of resonance radiation by Hg vapor is so great, the number of quanta absorbed in any of the experiments may be taken as equal to the number of quanta entering the reaction vessel. If the intensity may be considered constant, then the quantum yield may be known for any experiment provided a determination of the incident quanta has once been made.

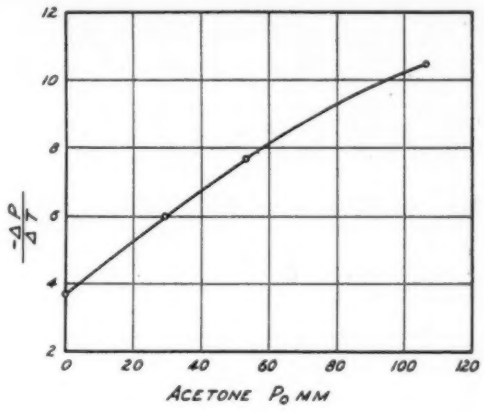

FIG. 3. The initial rate *vs.* the initial acetone pressure for an initial butadiene pressure of 190 mm.

A determination of the incident quanta was made using uranyl oxalate as an actinometer.[6] The reaction vessel was filled with a solution containing 0.01 mole per liter uranyl oxalate and 0.05 mole per liter oxalic acid. After a known period of irradiation an aliquot of the solution was titrated with standard 0.1*N* potassium permanganate. The intensity of light entering the reaction cell was found to be 4.2×10^{-4} einstein per minute. From the total volume of the system, 243 ml, and the rate of polymerization one obtains the expression for the quantum yield, $\Phi = -\Delta P/\Delta t \times 0.034$.

For the lowest pressure studied, 53 mm, this leads to a quantum yield of 0.24. Gee[4] has obtained a value of 0.2 for a pressure of 10 mm and a temperature of 15°C and Gunning and Steacie report 0.8 ± 5 for a pressure of 25 mm and a temperature of 30°C.

The Reaction Products

The principal reaction product has the appearance of a light yellow oil. This is somewhat soluble in benzene. In addition some white solid polymer insoluble in benzene is also formed. This polymer was removable only when heated in an oxygen stream. When there is no pressure change in the system on two successive readings, there is

[6] W. G. Leighton and G. S. Forbes, J. Am. Chem. Soc. **52**, 3139 (1930).

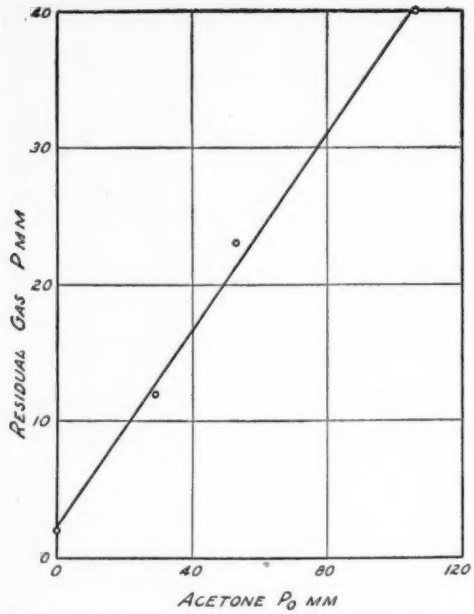

FIG. 4. Yield of gaseous products for experiments with constant initial butadiene pressure.

a residual gas which is not condensed at liquid-air temperature. For butadiene alone it has been shown that this gas is hydrogen.[4,5] For mixtures of butadiene and acetone, the uncondensable residue is much larger than for butadiene alone. In Fig. 4 the connection between this final residual pressure and the acetone concentration is shown. The linear relationship points to acetone as the source of this uncondensable residue. Carbon monoxide is formed when acetone is photolyzed,[7] and it is very probable that this is the gas formed in these experiments when acetone is present.

Detection of Free Radicals by the Metal Mirror Method

To determine whether free radicals are formed in the system C_4H_6, Hg, 2537A, the metallic mirror technique was used. Butadiene saturated with mercury vapor at room temperature was irradiated at a pressure of about 2.5 mm. The products passed over antimony mirrors which were readily removed. When acetone was substituted for butadiene, the same results were obtained. By measuring the time of mirror removal as a function of distance of irradiation zone from mirror, it was found that the half-life of free radicals from butadiene was about the same as for acetone.

Using the guard mirror methods developed by Burton[8] a search was made for H atoms in the irradiation products. The fragments were first passed over lead mirrors and then over antimony mirrors. Since lead will react with free radicals containing carbon but not with H atoms, the removal of antimony mirrors which will react with either is a criterion for the presence of H atoms if carbon containing radicals are first removed by lead mirrors. With these experimental conditions no evidence for the presence of H atoms was found.

Discussion

The findings of this study are in good agreement with the results obtained by Gunning and Steacie.[5] For butadiene alone, the existence of an apparent inhibition at the start of the run, the lessening of this inhibition, and an increased rate at lower pressures have been confirmed. The effect of adding acetone in this work has been found to be analogous to the addition of hydrogen in the work of Gunning and Steacie. However, the result of our mirror experiments demonstrating the absence of H atoms at low pressures leads to a modified interpretation of the mechanism. The results of Gunning and Steacie and the results reported herein are not in agreement with the work presented by Gee on the effect of pressure on the rate, the effect of hydrogen on the rate, and the interpretation of the inhibition. For this reason the discussion of the mechanism will be based on the suggestions already made by Gunning and Steacie.

The initial absorption act may be represented by

$$\mathrm{Hg}(^1S_0)+h\nu\rightarrow\mathrm{Hg}(^3P_1). \qquad (1)$$

TABLE I. Polymerization rate initiated by acetone.

Initial pressures Bu	Initial pressures Acetone	Mole fractions Bu	Mole fractions Acetone	Reaction rates, (mm/min.) Total	Reaction rates, (mm/min.) butadiene only	Reaction rates, (mm/min.) Acetone initiated
212	0	1	0	3.38	3.38	0
203	29	0.875	0.125	6.02	2.96	3.06
183	54	0.772	0.228	7.70	2.61	5.09
182	106	0.634	0.368	10.53	2.14	8.39

[7] G. H. Damon and F. Daniels, J. Am. Chem. Soc. **55**, 2363 (1933).

[8] M. Burton, J. Am. Chem. Soc. **58**, 1656 (1936).

The low quantum yield of the reaction and the effect of pressure on the rate indicate that the next step is the formation of an activated molecule,

$$Hg(^3P_1)+C_4H_6\rightarrow C_4H_6^*+Hg(^1S_0), \quad (2)$$

and that deactivation by collisional processes play an important role,

$$C_4H_6^*+M\rightarrow C_4H_6+M, \quad (3)$$

where M represents another molecule or the walls of the reaction vessel.

To explain the inhibition at the start of the reaction, the effect of pressure on the inhibition period, and the effect of added hydrogen on the rate, Gunning and Steacie have proposed the following sequence,

$$C_4H_6^*\rightarrow C_4H_4+H_2, \quad (4)$$

$$H_2+Hg(^3P_1)\rightarrow 2H+Hg(^1S_0), \quad (5)$$

$$C_4H_6+H\rightarrow C_4H_7, \quad (6)$$

$$C_4H_7+C_4H_6\rightarrow C_8H_{13}, \text{ etc.} \quad (7)$$

Reactions (5), (6), and (7) explain the effect of adding hydrogen on the rate very satisfactorily. However reaction (4) indicates that hydrogen formation is favored by low pressures and that the polymerization at low pressures occurs by an H-atom mechanism. In the mirror experiments, the presence of alkyl radicals and the absence of H atoms have been demonstrated. This leads to the conclusions that at low pressures the polymerization is induced by alkyl radicals and that hydrogen formation is favored by increasing the pressure. The following sequence is in accord with these conclusions:

$$C_4H_6^*+C_4H_6\rightarrow C_4H_4+H_2+C_4H_6, \quad (8)$$

$$C_4H_6^*\rightarrow 2C_2H_3, \quad (9)$$

$$C_4H_6+C_2H_3\rightarrow C_6H_9, \text{ etc.} \quad (10)$$

Reaction (9) may be considered to be a type of predissociation which would be favored by low pressures since it is in competition with reactions (3) and (8) which are favored by high pressures. Reaction (4) is now eliminated from consideration. Although reactions (5)–(10) may be going on at all pressures, the predominant mechanism at high pressures would be through the series (8), (5), (6), (7) while at low pressures the sequence (9), (10) would predominate. The evidence for C_4H_4 which is shown in reaction (8) is given in the paper by Gunning and Steacie.

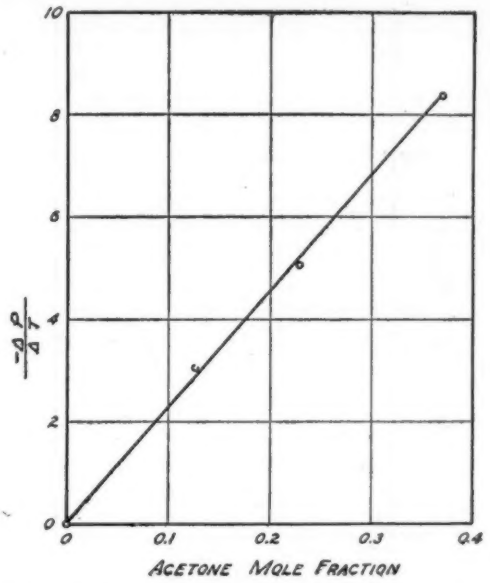

FIG. 5. Rate of polymerization induced by acetone.

A consideration of the sequence involving hydrogen indicates that until the hydrogen pressure is built up to the point where reaction (5) can take place to an appreciable extent, the apparent polymerization rate will be low because of the formation of hydrogen gas.

Gunning and Steacie have already explained the falling off of the rate at pressures below 2 mm as caused by incomplete quenching of activated mercury atoms. Thus the reaction

$$Hg(^3P_1)\rightarrow Hg(^1S_0)+h\nu \quad (11)$$

can occur at low enough pressures. This appears to be an adequate explanation.

The results obtained for added acetone are comparable to those obtained by Gunning and Steacie for added hydrogen. The equations necessary are,

$$(CH_3)_2CO+Hg(^3P_1)\rightarrow CH_3+CH_3CO+Hg(^1S_0), \quad (12)$$

$$CH_3CO\rightarrow CH_3+CO, \quad (13)$$

$$CH_3+C_4H_6\rightarrow C_5H_9, \text{ etc.}, \quad (14)$$

$$CH_3CO+C_4H_6\rightarrow C_5H_9CO, \text{ etc.} \quad (15)$$

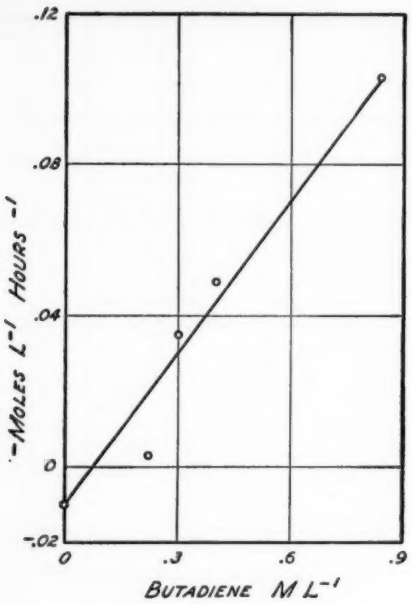

FIG. 6. The initial rate *vs.* the initial butadiene concentration for an initial acetone concentration of 0.23*M*.

Reactions (12) and (13) may be deduced from what is already known of the radicals formed from acetone.[9] Since only about 40 percent of the possible CO is accounted for by the uncondensed gas formed, CO may enter the polymer through such a reaction as (15). In addition to these reactions, it is quite probable that alkylation of the polymer can occur after the butadiene concentration is reduced sufficiently. The shape of curve *d*, Fig. 1, suggests such a reaction, the steepest linear portion being attributed to polymerization while the curved portion represents an alkylation of the polymer. This curved portion is much more marked than may be attributed to a reduction of incident light intensity by the deposition of polymers on the quartz surface.

Although no data on the quenching of activated mercury by acetone or butadiene are known, it might be expected that they would have comparable quenching diameter. Since their molecular weights are very close together, 54 and 58, the amount of energy transferred from mercury to either molecule would be proportional to its mole fraction. If it is further assumed that the process for the mixture may be separated into two parts, one initiated by energy transferred to butadiene and the other initiated by energy transferred to acetone, then it is possible to calculate the part due to acetone. Table I and Fig. 5 show the results obtained.

The straight line obtained in Fig. 5 indicates that the rate of polymerization induced by acetone is directly proportional to the number of free radicals formed from acetone. This is a very interesting result as it suggests that the termination of the polymerization chain is not caused by the interaction between free radicals and that the termination step is first order with regard to free radicals. It may be observed that a similar suggestion with regard to butadiene alone has been made.[4]

A crude estimate of the average polymer chain length may be made from the above data. From the values of quantum yield given for acetone photolysis,[7] the quantum yield of free radical production from acetone may be taken as 0.2 ± 0.1 for the conditions of these experiments. From the actinometric determination and from the data of Table I, the quantum yield of the acetone induced part of the reaction is calculated to be 0.8. This gives, as the number of molecules reacting per free radical, the value $0.8/(0.2\pm0.1)$, or between 3 and 8 molecules per chain as the average length.

PART II. THE REACTION OF BUTADIENE-ACETONE MIXTURES IN HEXANE SOLUTION

Solutions of butadiene and acetone in hexane were irradiated in a quartz tube 20×250 mm. The tube was quartz jacketed and thermostated water at 25° circulated through the jacket. The entire assembly fitted inside the helical mercury resonance lamp. Irradiation was carried out for 10-minute periods.

The butadiene content of the solution was determined by removing 1.00-ml aliquots and adding an excess of ICl solution in carbon tetrachloride. The solution was allowed to stand 30 minutes in the dark; an excess of 10 percent KI solution was added and the liberated iodine was titrated with 0.1*N* sodium thiosulfate until the CCl_4 layer became colorless. It was assumed that addition occurred on all of the double bonds and that each butadiene molecule which entered into a polymerization reaction lost one double bond.

[9] H. H. Glazebrook and T. G. Pearson, J. Chem. Soc., 567 (1937).

Figure 6 shows the results obtained when the initial polymerization rate is plotted against the initial butadiene concentration for a constant initial acetone concentration. The effect of varying the initial acetone concentration for a constant initial butadiene concentration is shown in Fig. 7. An apparent negative polymerization means an increase in the double bond character of the solution. This may be attributed to the fact that unsaturated molecules are formed when ketones alone are irradiated.[3]

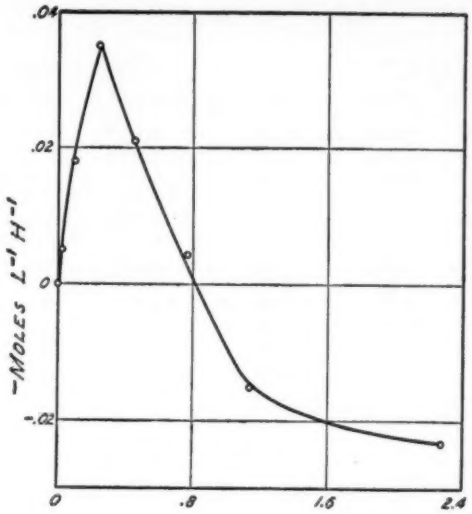

FIG. 7. The initial rate *vs.* the initial acetone concentration for an initial butadiene concentration of 0.30*M*.

Discussion

To explain the low quantum yield of many photochemical reactions in liquid solution, Franck and Rabinowitch[10] have postulated that recombination of primary free radicals plays an important role. Thus when free radicals are formed in a cage of solvent molecules, if they cannot react with solvent molecules then, except for free radicals which have enough energy to escape the solvent cage, the principal reaction is a recombination of the radicals. Atwood and Rollefson[11] have pointed out that an equivalent concept is the formation of an activated molecule which can lose its energy by collision with solvent molecules until there is insufficient energy to break a bond, and hence free radicals are not formed. From this point of view, the initial absorption act for acetone is

$$(CH_3)_2CO+h\nu\rightarrow(CH_3)_2CO^*, \quad k_1. \qquad (16)$$

The activated molecule formed may be considered to be in a state of collision with one of the 3 substances, acetone, butadiene, or hexane. Let it now be postulated that collision with hexane molecules results in deactivation,

$$(CH_3)_2CO^*+C_6H_{14}\rightarrow (CH_3)_2CO+C_6H_{14}, \quad k_2. \qquad (17)$$

Now when there is a possibility of reaction between the activated species and another molecule, then the collision may be considered to result in free radicals even though it is realized that at least one of the free radicals formed is instantaneously removed by reaction. If it is assumed that collision between activated acetone and either butadiene or another acetone molecule results in reaction, then the equations may be written

$$(CH_3)_2CO^*+C_4H_6\rightarrow 2CH_3+CO+C_4H_6, \quad k_3 \qquad (18)$$

$$(CH_3)_2CO^*+(CH_3)_2CO\rightarrow 2CH_3+CO+(CH_3)_2CO, \quad k_4 \qquad (19)$$

followed by,

$$CH_3+C_4H_6\rightarrow C_5H_9, \quad k_5 \qquad (20)$$

$$C_5H_9+(n-1)C_4H_6\rightarrow C_5H_9(n-1)C_4H_6, \quad k_6 \qquad (21)$$

and,

$$CH_3+(CH_3)_2CO\rightarrow \text{unsaturated molecule}+\cdots k_7. \qquad (22)$$

This sequence accounts for the main features of Fig. 7. The initial rise in polymerization rate with increasing acetone concentration is attributed to an increase in the amount of light absorbed. It may be calculated that a 1-cm layer of hexane solution 0.25*M* in acetone will absorb more than 95 percent of incident 2537A radiation. The subsequent decrease and finally apparent negative polymerization with increasing acetone concentration can be accounted for by reaction (22) which is considered to yield unsaturated compounds. This differs from the interpre-

[10] J. Franck and E. Rabinowitch, Trans. Faraday Soc. **30**, 120 (1934).
[11] K. Atwood and G. K. Rollefson, J. Chem. Phys. **9**, 506 (1941).

TABLE II. Calculated rates of polymerization.

Concentration, moles/liter Butadiene	Acetone	$\frac{I_{abs}}{I_0}$	Polymerization rate, moles/liter/hour Experimental	Calculated
0.30	0.023	0.40	0.0052	0.016
0.30	0.091	0.86	0.018	0.028
0.30	0.23	1.00	0.035	0.035
0.30	0.45	1.00	0.021	0.026
0.30	0.68	1.00	0.0041	0.017
0.30	1.20	1.00	−0.015	0.004
0.30	2.20	1.00	−0.023	−0.035
0.00	0.23	1.00	−0.01	−0.008
0.21	0.23	1.00	+0.004	+0.021
0.30	0.23	1.00	+0.035	+0.035
0.40	0.23	1.00	+0.049	+0.049
0.84	0.23	1.00	+0.12	+0.11

tation of Norrish[3] that unsaturated molecules would result from interaction with hexane.

The apparent rate of polymer formation then becomes the rate at which C=C bonds are removed less the rate at which they are formed. Using the steady-state treatment for activated molecules and free radicals this becomes

$$dP/dt = nk_5[CH_3][C_4H_6] - k_7[CH_3][(CH_3)_2CO]. \quad (a)$$

Let

$$[C_4H_6]=A, \quad [(CH_3)_2CO]=B, \quad [C_6H_{14}]=C.$$

Then

$$\frac{dP}{dt}=\frac{k_1 I_{abs}(nk_5A-k_7B)(2k_3A+2k_4B)}{(k_5A+k_7B)(k_3A+k_4B+k_2C)}. \quad (b)$$

Assuming $k_2=k_3=k_4$, $k_5=k_7$ and that the total concentration $A+B+C$ is a constant, this may be written

$$\frac{dP}{dt}=\frac{kI_{abs}}{I_0}(n[C_4H_6]-[(CH_3)_2CO]). \quad (c)$$

I_{abs}/I_0 may be calculated from the law of Lambert and Beer, $I_{abs}/I_0=l-10^{-\epsilon Cl}$. We may use for l the average length of light path or for a cylinder 20 mm in cross section take $l=12$ mm, the average chord length for a circle 20 mm in diameter. The value of ϵ in hexane at 2537A is 8.0.[12] If values are assigned to k and n it is now possible to calculate the polymerization rate from Eq. (c). In Table II such a calculation has been made for the experimental points of Figs. 6 and 7. Here n, the average chain length, has been taken as equal to 4 and k has been assigned the value 0.035.

Considering the nature of the approximation involved in obtaining the final rate equation and the effective I_{abs}/I_0 values, the extent of agreement obtained seems significant. It may be observed that the value of average chain length used, 4, is within the limits previously derived for the gas phase polymerization. Again no explanation for the chain breaking step is given but it is implied that it does not occur by interaction between free radicals.

ACKNOWLEDGMENT

The author wishes to thank Professor Laitenen for helpful suggestions in regard to the analysis of butadiene in solution and Professors Rodebush, Wall, and Marvel for their interest in the work.

[12] *International Critical Tables* **5**, 371 (1929).

An Electron Diffraction Investigation of Dimethylketene Dimer*

WILLIAM N. LIPSCOMB AND VERNER SCHOMAKER
Department of Chemistry, California Institute of Technology, Pasadena, California

(Received April 17, 1946)

An electron diffraction investigation of dimethylketene dimer confirms the 2,2,4,4-tetramethylcyclobutadione-1,3 structure. The following parameters were determined for the symmetrical model: C−C (ring) = 1.56±0.05A, C−CH_3 = 1.54±0.05A, C=O = 1.22±0.04A, ∠C−CO−C = 93°±6°, and ∠CH_3−C−CH_3 = 111°±6°. The limits of error assigned to the angles apply only if simultaneous variation is excluded; otherwise much larger limits must be assigned. A notable feature of the structure is the large temperature factor which must be ascribed to the interatomic distances greater than 3A. The relation of this temperature factor to the unusually large atom polarization is discussed in terms of the probable amplitudes of the pertinent modes of vibration of the molecule.

THIS investigation of the molecular structure of dimethylketene dimer, which may be presumed to be 2,2,4,4-tetramethylcyclobutadione-1,3, was undertaken because of its interest in connection with the structure of diketene, which is still under active discussion. Although work on diketene was begun, it was discontinued because our diffraction photographs were unsatisfactory and because it was understood that an electron diffraction investigation is forthcoming from another laboratory.[1]

EXPERIMENTAL

The sample of dimethylketene dimer was prepared by Dr. C. W. Smith of the Shell Development Company, Emeryville, California. Dimethylketene [$(CH_3)_2C=C=O$], prepared from α-bromoisobutyryl bromide, was isolated and then allowed to polymerize in ethyl acetate solution. The dimethylketene dimer which was separated from this mixture melted at 113°–114°C. A rough determination of its vapor pressure gave the values 6 mm at 52°C and 38 mm at 87°C. These characteristics are in agreement with those reported[2,3] in the literature for samples obtained by different syntheses. As might be expected the compound has no permanent dipole moment.[2,3] Diketene, on the other hand, has a dipole moment[4] of 3.31 D, and so cannot have the cyclobutadione-1,3 structure.

The electron diffraction investigation was carried out with the apparatus described by Brockway.[5] Photographs were taken at a camera distance of 10.93 cm with electrons of wavelength 0.0610A as determined by standardization against zinc oxide.[6] The vapor was obtained from a sample of the substance heated at 90° to 120°C in a high temperature nozzle.[7]

INTERPRETATION

Both the radial distribution method[8] and the correlation method[9] were used in interpreting the photographs. The radial distribution function was calculated[10] from the visual intensity curve by means of the equation

$$rD(r) = \sum_{q_i = 1, 2, \cdots, 100} I(q_i) \times \exp(-aq_i^2) \sin\left(\frac{\pi}{10} q_i r\right), \quad (1)$$

with a so determined that $\exp(-aq_i^2)$ is equal to 0.10 at $q = 90$. The theoretical intensity curves used in the correlation treatment were calculated

* Contribution from the Gates and Crellin Laboratories of Chemistry, California Institute of Technology, Pasadena, California, No. 1060.

[1] S. H. Bauer, private communication.

[2] D. Hammick, G. C. Hampson, and G. I. Jenkins, J. Chem. Soc. 1263 (1938).

[3] I. E. Coop and L. E. Sutton, J. Chem. Soc. 1269 (1938).

[4] P. F. Oesper and C. P. Smyth, J. Am. Chem. Soc. **64**, 768 (1942).

[5] L. O. Brockway, Rev. Mod. Phys. **8**, 231 (1936).

[6] C. S. Lu and E. W. Malmberg, Rev. Sci. Inst. **14**, 271 (1943).

[7] L. O. Brockway and K. J. Palmer, J. Am. Chem. Soc. **59**, 2181 (1937).

[8] L. Pauling and L. O. Brockway, J. Am. Chem. Soc. **57**, 2684 (1935).

[9] L. Pauling and L. O. Brockway, J. Chem. Phys. **2**, 867 (1934).

[10] R. Spurr and V. Schomaker, J. Am. Chem. Soc. **64**, 2693 (1942).

from the simplified formula[10]

$$I^0(q)=\sum_{i,j}\frac{Z_iZ_j}{r_{ij}}\exp(-b_{ij}q^2)\sin\left(\frac{\pi}{10}r_{ij}q\right), \quad (2)$$

where the constant b_{ij} in the exponential temperature factor term was given the value 0.00015 for bonded C−H terms, 0.0003 for non-bonded C···H terms, and 0 for all other terms.

RESULTS

The electron diffraction pattern of dimethylketene dimer is represented by curve *V* of Fig. 1. The unobservable first feature (dotted portion of curve *V*), which is relatively insensitive to structure, was taken from the theoretical curves. The radial distribution function *R* calculated from this visual curve shows sharp peaks at 1.17A, 1.55A, 2.20A, and 2.58A, and rather broad peaks at 3.32A and at 4.43A. Its interpretation in terms of the tetramethylcyclobutadione structure is straightforward. The first peak corresponds to the C−H and C=O terms; with the assumptions that the C−H peak is at 1.09A, that it corresponds to a temperature factor with $b_{C-H}=0.00015$, and that the two terms have the relative weights corresponding to those expected for tetramethylcyclobutadione, this first peak gives a C=O distance of about 1.22A. The peak at 1.55A corresponds to the C−C distances in the four-membered ring and to the C−CH_3 distances. These distances cannot differ greatly because the half-width (at half-height) of this peak corresponds closely with that expected from the use of the exponential term in Eq. (1), namely, $w_l=8.5/q_{max}$. The peak at 2.20A corresponds to the non-bonded C···H terms and the cross-ring C···C distances. Analysis of this peak with the assumptions C···H=2.16A and $b_{C\cdots H}=0.0003$ yields a C···C distance of 2.21A, which corresponds to a C−C bond distance of 1.56A in the ring, in good agreement with the 1.55A peak. (A strict interpretation would then suggest a C−CH_3 distance of 1.54A.) The peak at 2.58A corresponds to the shortest non-bonded C···O, C···CH_3, and CH_3···CH_3 distances, which have relative weights nZ_iZ_j/r_{ij} of 20, 30, and 8. With consideration of the small width of this peak, these distances, particularly the first two, cannot differ greatly from 2.58A. The remaining comparisons of the distance spectrum of tetramethylcyclobutadione with the radial distribution function (as shown for model *A*; see Fig. 1) is satisfactory if the terms corresponding to distances greater than 3A are given suitable temperature factors. Thus the terms which contribute to

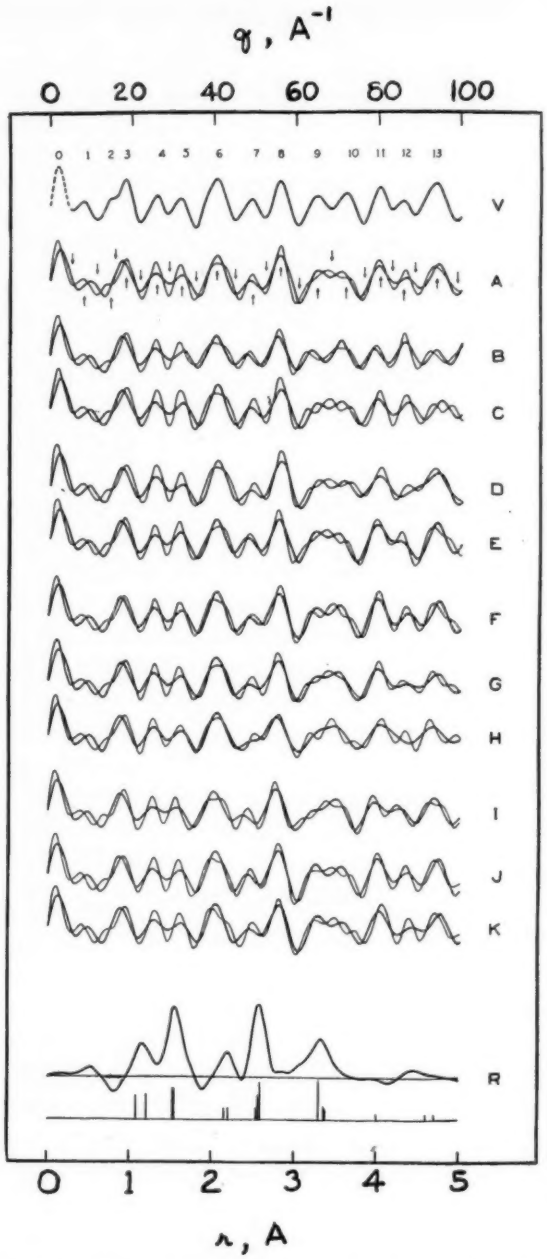

FIG. 1. Electron diffraction curves for dimethylketene dimer: visual curve *V*, theoretical intensity curves *A*···*K*, and radial distribution function *R*. The heavy theoretical curves were calculated (for models defined in the text) omitting distances greater than 3A; in the light curves all distances were included. The numbers above curve *V* and the arrows on curve *A* refer to the measured *q* values in Table I.

the peak at 3.32A give a composite term at 3.33A, in good agreement with the position and also with the area of this peak, but if the temperature factor is omitted the resulting peak is too narrow and too high as compared with that shown by the radial distribution function. The small peak at 4.43A does not correspond well with the spectrum of the comparatively unimportant long distances in the molecule, but it may indicate in a general way the presence of scattering from these terms. At any rate it can be said that the discrepancies in this region represent errors in the visual curve no greater in magnitude than those demonstrated by the two sharp negative regions at 0.83A and 1.89A, and that the tetramethylcyclobutadione structure is well confirmed by the radial distribution curve.

In the correlation procedure the visual curve was compared with theoretical intensity curves calculated for tetramethylcyclobutadione models of symmetry D_{2h} (except for the hydrogen atoms) with the bonded C−H distance 1.09A and tetrahedral bond angles at the methyl carbon atoms. All hydrogen interaction terms except those due to the bonded and shortest non-bonded carbon-hydrogen distances were omitted, because of their relatively small weight and necessarily severe temperature factors. The five parameters of this structure may be taken as the ratio $(C-C)/(C-CH_3)$, the ratio $2(C=O)/[(C-C)+(C-CH_3)]$, the C−CO−C (ring) angle, the CH_3-C-CH_3 angle, and as size parameter, $[(C-C)+(C-CH_3)]/2$. The temperature factor for the distances greater than 3A also needs to be determined. In order to take account of this temperature factor two theoretical curves were calculated for each model, only the terms less than 3A being included for the additional, heavy curve (Fig. 1). It was found that for the best models the most satisfactory agreement with the visual curve was obtained by interpolation[11] between the heavy and light curves according to the temperature factor $\exp(-b_{ij}q^2)$ for distances greater than 3A with b_{ij} equal to 0.0006. An upper limit of $b_{ij}=0.0008$ can be determined by the requirement that the second maximum (Fig. 1) be adequately resolved from the third maximum, while a lower limit of $b_{ij}=0.0004$ may be arrived at by the requirements that the fourth and fifth maxima be somewhat weak as compared with the sixth maximum, and that the ninth and tenth maxima shall remain two resolved peaks of approximately equal intensity instead of becoming a triple peak. On the basis of these considerations and the analysis of the width of the 3.3A peak of the radial distribution function in terms of the distances for the various models and the temperature factor, we believe that the value of $b_{ij}=0.0006$ cannot be in error by more than about ±30 percent.

Model *A*, which was suggested by the radial distribution function, is defined by the parameters $2(C=O)/[(C-C)+(C-CH_3)]=1.22/1.55$, $(C-C)\text{ ring}/(C-CH_3)=1.56/1.54$, $\angle C-CO-C$ (ring) $=90°$, $\angle CH_3-C-CH_3=109°\ 28'$, and $[(C-C)+(C-CH_3)]/2=1.55$A, and leads to curves *A* in excellent agreement with the visual curve *V* in the sense of the interpolation just described. The slight discrepancy in regard to the relative intensities of the ninth and tenth maxima is discussed below. Re-examination of the photographs indicated that the differences in the third, fourth, fifth, and sixth maxima were exaggerated slightly in the drawing of the visual curve, and that the interpolated theoretical curve is actually in good agreement with the photographs in these respects.

A complete examination of all possible parameter variations in the neighborhood of model *A* was not undertaken, although each of the parameters was varied separately in the following series of models, in which, unless otherwise stated, the parameters have the same values as in model *A*. In considering the effects on the curves of parameter variation it was found useful throughout to think in terms of the radial distribution function. Variation of $(C-C)/(C-CH_3)$ to 1.61/1.49 and to 1.51/1.59 is illustrated by curves *B* and *C*; it appears that for this variation models with these two distances differing by as much as 0.09A are definitely inacceptable, particularly with regard to the relative intensities of the extreme outer features. Models *D* and *E*, with $2(C=O)/[(C-C)+(C-CH_3)]$ equal to

[11] The interpolated curve lies 13 percent of the way from the light toward the heavy curve at $q=15$; 42 percent at $q=30$; and 95 percent at $q=70$. For the best model the three distances contributing to the 3.3A peak are nearly equal. Some of the less satisfactory models tend to require somewhat different values of b_{ij}; for example, models with these distances distributed about 3.3A as an average require smaller values of b_{ij}.

1.17/1.55 and 1.27/1.55 are somewhat outside of the range of acceptability. Of the three models, *F*, *G*, and *H*, in which the C−C−C angle at the carbonyl group was given the values 85°, 95°, and 100°, *F* and *G* are nearly acceptable, while *H* is definitely poor. Of models *I*, *J*, and *K*, in which the CH_3-C-CH_3 angle was given the values 100°, 115°, and 120°, the only acceptable model is *J*.

Simultaneous variations of the parameters were investigated by inspection of the curves on the assumption that the effects of the variations are additive, as they must be for small variations. Combinations of variations of $(C-C)/(C-CH_3)$ and $2C=O/[(C-C)+(C-CH_3)]$ do not lead to better agreement than that shown in curve *A*, as may be seen by comparisons of curves *B*, *C*, *D*, and *E*; neither do they suggest that simultaneous variations of these parameters could lead to satisfactory models with parameters outside the ranges of acceptability established for the single variations. The same is true, moreover, for combined variations of these two parameters with either one of the angles. However, when simultaneous variations of the two angles are allowed a much increased range of acceptable angle values is revealed in which the angles are increased or decreased together. This is illustrated by an average of curves *G* and *J* with somewhat the greater weight for *G*. Indeed, slightly better agreement with the relative intensity of the ninth and tenth maxima than shown by model *A* is obtained by a variation in the direction of this combination without producing unsatisfactory effects elsewhere. On the other hand, simultaneous increase of one angle and decrease of the other leads very quickly to unsatisfactory curves.

On the basis of the radial distribution function, these considerations, and quantitative comparison of observed and calculated q values for models *A* (Table I), *C*, *E*, *G*, and *J* the final parameters were taken as $C-C=1.56$A, $C-CH_3=1.54$A, $C=O=1.22$A, $\angle C-CO-C=93°$, and $\angle CH_3-C-CH_3=111°$. Although the average of C−C and $C-CH_3$, which determine the position of the 1.55A peak of the radial distribution function, can be determined with the usual precision (±0.02A), their difference cannot, the two distances being so nearly alike as to be unresolvable; this circumstance makes it necessary to assign the considerably larger value ±0.05A for the limits of error (limits which we believe the error is not likely to exceed) of the separate determination of these two distances. The C=O distance, with the limits of error of ±0.04A, is also not well fixed because all of the oxygen terms are either unimportant or imperfectly resolved from other terms. Limits of ±6° can be assigned to the angle variations if simultaneous variation of the two angles is excluded; otherwise much greater limits of error, so great as almost to deprive the experimental values of any quantitative significance, must be assigned.

TABLE I.

Min.	Max.	q obs.	q calc.[a]	q calc./q obs.
1		5.32	5.5	(1.034)
	1	8.25	8.1	(0.982)
2		11.60	11.4	(0.983)
	2	14.81	14.7	(0.993)
3		16.13	15.6	(0.967)
	3	18.58	18.5	0.996
4		22.07	22.0	0.997
	4	26.09	25.8	0.989
5		28.68	28.8	1.004
	5	31.87	31.8	0.998
6		35.35	35.5	1.004
	6	40.64	40.7	1.001
7		44.95	45.5	1.012
	7	49.15	49.1	0.999
8		52.41	51.8	0.988
	8	55.90	55.9	1.000
9		60.50	60.5	1.000
	9	65.02	65.2	1.003
10		68.37	68.0	0.995
	10	72.02	70.9	0.984
11		76.30	75.3	0.987
	11	80.28	80.0	0.997
12		83.24	83.9	1.008
	12	86.06	86.7	1.007
13		88.66	90.0	1.015
	13	93.94	94.3	1.004
14		98.91	98.9	1.000
			Average	0.999
			Average deviation	0.006

[a] The values of q_{calc} were taken from the average curve obtained by weighting the light and heavy curves of model *A* according to the factor $\exp(-0.0006q^2)$. Values in parentheses were omitted in the calculation of the average and average deviation.

TEMPERATURE FACTOR AND ATOM POLARIZATION

The tetramethylcyclobutadione molecule is so complex that any simple consideration of the vibrations responsible for the anomalously large temperature coefficient, which represents an increment to the average that prevails for the shorter distances in the molecule, is likely to be unsatisfactory. Indeed, our estimate of the temperature factor coefficient is not itself very precise. We wish, nevertheless, to discuss a

particular mode of vibration which we believe may be mainly responsible both for the anomalous temperature factor of the longer distances and the unusually large atom polarization,[3] which corresponds to a root-mean-square dipole moment of about 0.7 D. Coop and Sutton[3] concluded that a mode of vibration different from that which we propose was responsible for the anomalous atom polarization. For each of these two modes of vibration we shall compare the root-mean-square amplitude required for the anomalous temperature factor, and that required for the anomalous atom polarization, with estimates of the amplitudes to be expected on the basis of classical temperature excitation.

The first-mentioned mode of vibration is the one in which, approximately, the $\diagdown C{=}O \diagup$ groups oscillate in a plane perpendicular to that of the ring while the $\diagdown C(CH_3)_2 \diagup$ groups move similarly and in the opposite direction, each of the groups retaining its two planes of symmetry and the four bond angles in the ring remaining equal. If the coefficient $b_{ij}=0.0006$ can be said to apply to the $CH_3\cdots O$ distances, as is reasonable since these are by far the most important of the long distances, for which b_{ij} was derived as an average[12] value, the root-mean-square deviation, θ, of the C=O bonds from the mean plane of the molecule, is 5°. The atom polarization of the gas molecule corresponds to a root-mean-square dipole moment of 0.66 D. Reduced to 0.6 D to allow for the "normal" atom polarization (5 percent of P_E) which might be expected for the simpler group vibrations, this moment corresponds to a value of 7° for θ, in fair agreement with the diffraction data estimate. That these amplitudes are reasonable for this mode of vibration can be seen from a calculation of the amplitude for classical excitation at 100°C on the assumption of a parabolic potential function[13] for bending of the ring bond angles from an (assumed) normal angle ϑ_0 of 109½°. This amplitude, $\theta=3.5°$, is smaller than the values derived above. It may be remarked, however, that the expected anharmonicity of the potential function would lead to a considerable increase of the estimate, the ring bond angles being greatly strained from their normal tetrahedral values.

Coop and Sutton[3] attributed the atom polarization predominantly to oscillations of the C=O groups in the plane of the four-membered ring. In order to account for the b_{ij} value of 0.0006 by this mode of vibration alone a root-mean-square displacement, θ', of the C=O bond of 14° is required. The anomalous atom polarization requires a value of θ' of 10° if the two C=O groups are assumed to oscillate independently. With the assumption of a constant of 10^{-11} erg/radian^2 for bending the C=O bond against the rest of the C−CO−C group, the amplitude calculated for classical excitation is found[14] to be $\theta'=2°$.

These calculations show that the very large temperature factor for the long distances in dimethylketene dimer is of the right order of magnitude to be consistent with the anomalous atom polarization. They further suggest that both of these effects may well arise predominantly from an out-of-plane vibration of the ring atoms and the attached groups rather than from vibrations of the oxygen atoms in the plane of the ring as suggested by Coop and Sutton. To be sure the argument is based on force constant estimates which are none too reliable; however, it seems unlikely that they can be so greatly in error as to invalidate the conclusion.

ACKNOWLEDGMENT

We wish to thank Professor Linus Pauling for his interest and encouragement, and Dr. Robert Rasmussen of the Shell Development Company for his courtesy in providing us with the sample of dimethylketene dimer.

[12] Only the 3.3A group of distances is important. If for this group account were taken of the relatively small dependence of the $CH_3\cdots C$ (ring) and $O\cdots C$ (ring) distances on this vibration as compared with that of the $CH_3\cdots O$ distances this estimate of θ would be slightly increased; however, for a model with distances in the 3.3Å region not all alike (reference 11) it would be somewhat decreased.

[13] The constant $k=10^{-11}$ erg/radian^2/bond angle in the potential function $2V=k(\delta\vartheta_{C-C-C})^2$ was estimated from the bending frequency of propane.

[14] The bending constant used here for C=O against the C−C−C group suggests itself as a reasonable lower limit in view of the bond bending constants listed by Herzberg (*Infrared and Raman Spectra of Polyatomic Molecules* (D. Van Nostrand Company, Inc., New York, 1945), p. 193), at least if it is assumed that the bond angle strain in the four-numbered ring has no great effect on this constant. With this force constant the estimated frequency of the vibration is low enough (about 300 cm^{-1}) that the assumption of classical excitation cannot be greatly in error.

THE JOURNAL OF CHEMICAL PHYSICS VOLUME 14, NUMBER 8 AUGUST, 1946

The Determination of Critical Concentrations for the Formation of Soap Micelles by the Spectral Behavior of Pinacyanol Chloride*

M. L. CORRIN, H. B. KLEVENS, AND WILLIAM D. HARKINS
Department of Chemistry, University of Chicago, Chicago, Illinois

(Received May 8, 1946)

The absorption spectrum of pinacyanol chloride in aqueous solutions of anionic soaps changes sharply to that characteristic of its solutions in organic solvents over a short range of soap concentration. This effect is attributed to the formation of micelles, in whose hydrocarbon-like layers or cores the dye is solubilized. The concentration of soap at which this spectral change occurs is taken as "the critical concentration for the formation of micelles." In water the dye exhibits an absorption band at 5500A which disappears rapidly as the concentration of molecular soap increases. Thus, even 0.00006 molar potassium laurate gives a large effect. At about 0.0126 *M* the γ-band at about 4800A reaches a high intensity, which falls, with further increase of concentration, very rapidly close to the critical concentration. At 2.3 to 2.4×10^{-2} for potassium laurate and 6×10^{-3} for the myristate the α-band (*ca.* 6150A) and the β-band (*ca.* 5700A) begin to increase rapidly in intensity and these are considered as the critical concentrations, since these are the prominent bands in the solution of the dye in an oil. Alkali oleate and dilinoleate soaps exhibit an additional band (ω-band) at about 5200A. Some other critical concentrations determined by this method are $3.6–5.2\times10^{-4}$ molar for sodium cetyl sulfate, $2.5–3.2\times10^{-2}$ molar for potassium dehydroabietate, $7–12\times10^{-4}$ molar for potassium oleate, and 2.5×10^{-4} molar for potassium dilinoleate. The values for the last two soaps are uncertain, since their behavior differs considerably from that displayed by the salts of saturated acids. All measurements were made at 25.8°C with the exception of the sodium cetyl sulfate which was investigated at 35.8°C. An absorption band at approximately 4800A appears in all the soap solutions measured below the critical concentration with the exception of potassium dilinoleate. This band is absent when salts or bases are added to the dye solution. A titrametric method has been developed for the determination of critical concentrations of soaps in the presence of added salts and hydrocarbons.

AQUEOUS solutions of most soaps exhibit a more or less abrupt change in physical properties over a relatively short concentration range; this phenomenon has been attributed to the formation of oriented soap aggregates, and the concentration at which it occurs has been termed "the critical concentration for the formation of micelles." The nature of the transition taking place at the critical concentration is as yet unknown, and a controversy still exists concerning the possible existence of aggregates at lower concentrations. The structure of soap aggregates in the neighborhood of the critical concentration is also a matter of dispute.

The work in this field has been extensive, and no effort is made to cite all authors or publications. Thus, conductivity studies indicate a sharp change in slope when the equivalent conductance is plotted against the square root of the soap concentration; the effect has been reported for alkali salts of the aliphatic fatty acids,[1] long chain amine salts,[2] sulfonates,[3] and sulfates.[4] The concentration at which this change occurs is dependent upon the chain length of the detergent of a given type and, to a far less extent upon the temperature. Similar effects have been noted in studies of freezing point depression,[5] density,[6] surface tension-time effects,[7] viscosity,[8] and transference number.[9] For a given detergent at a given temperature the change in all such physical properties occurs at approximately the same concentration.

* The work reported in this paper was done in connection with the Government Research Program on Synthetic Rubber under contract with the Office of Rubber Reserve, Reconstruction Finance Corporation.

[1] (a) J. W. McBain, M. E. Laing, and A. F. Titley, J. Chem. Soc. **115**, 1279 (1919). (b) P. Ekwall, Kolloid Zeits. **101**, 135 (1942).

[2] A. W. Ralston and C. W. Hoerr, J. Am. Chem. Soc. **64**, 772 (1942).

[3] K. A. Wright, A. D. Abbott, V. Sivertz, and H. V. Tartar, J. Am. Chem. Soc. **61**, 549 (1939).

[4] A. Lottermoser and F. Puschel, Kolloid Zeits. **63**, 175 (1933).

[5] S. A. Johnston and J. W. McBain, Proc. Roy. Soc. **181**, 119 (1943).

[6] (a) C. R. Bury and G. J. Parry, J. Chem. Soc. 626 (1935). (b) K. A. Wright and H. V. Tartar, J. Am. Chem. Soc. **61**, 544 (1939).

[7] (a) N. K. Adam and H. L. Shute, Trans. Faraday Soc. **34**, 758 (1938). (b) G. C. Nutting, F. A. Long, and W. D. Harkins, J. Am. Chem. Soc. **62**, 1496 (1940). (c) H. V. Tartar, V. Sivertz, and R. E. Reitmeier, J. Am. Chem. Soc. **62**, 2375 (1940).

[8] K. A. Wright and H. V. Tartar, J. Am. Chem. Soc. **61**, 545 (1939).

[9] C. W. Hoerr and A. W. Ralston, J. Am. Chem. Soc. **65**, 976 (1943).

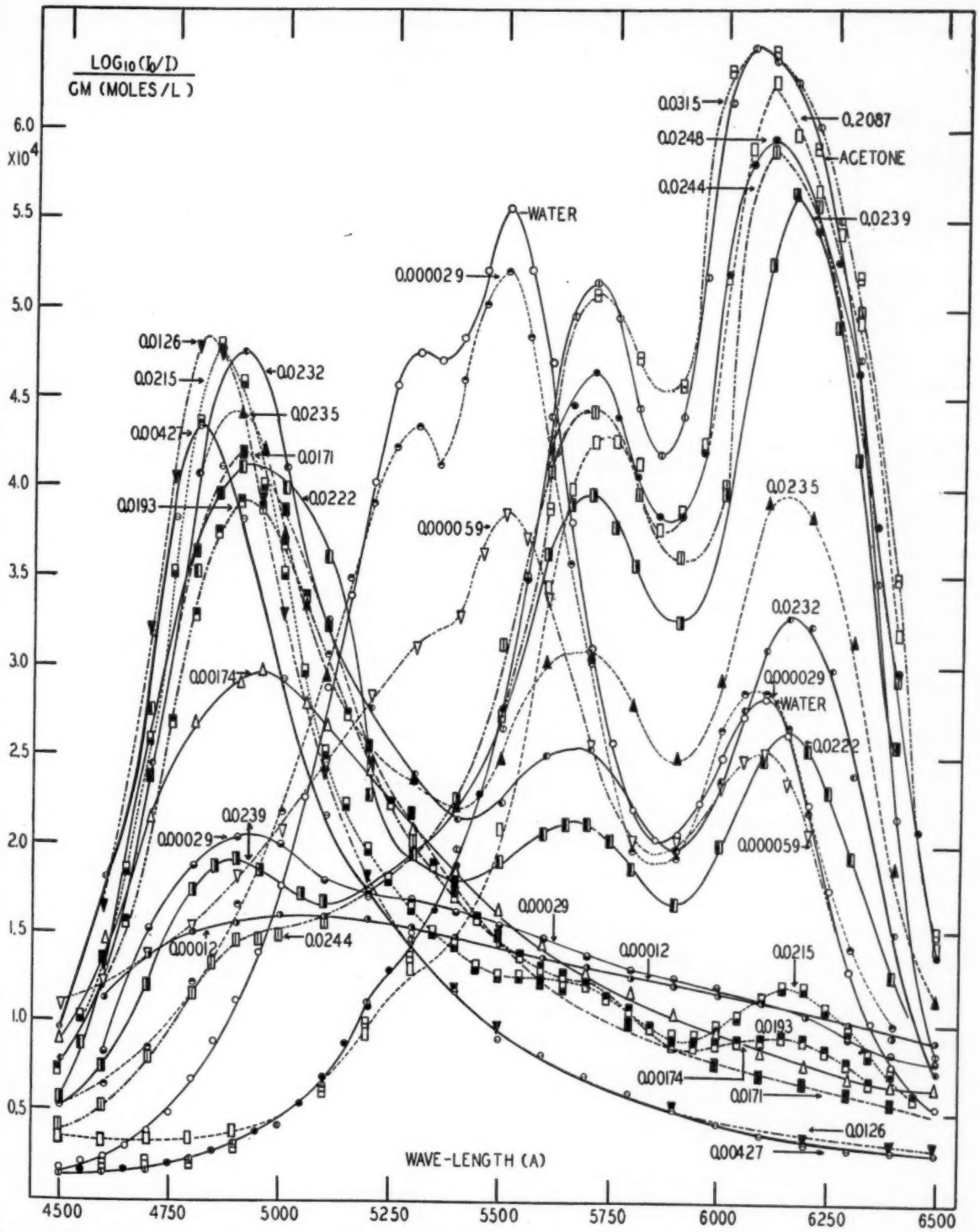

FIG. 1. Effect of varying potassium laurate concentration on the absorption spectra of 1×10^{-4} *M* pinacyanol chloride in aqueous solution.

It has been shown by Sheppard[10] that the absorption spectrum of pinacyanol chloride obeys Beer's law in organic media while deviating from such behavior in water. Furthermore, the over-all nature of the spectrum is markedly different for

[10] S. E. Sheppard, Rev. Mod. Phys. **14**, 303 (1942).

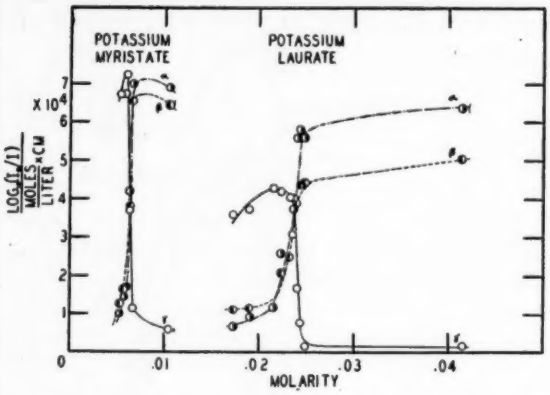

FIG. 2. Intensity of band maxima *versus* soap concentration for potassium laurate and myristate.

the dye in a non-polar environment than in water. This has been attributed to the existence of a dimerized form of the dye in water and the monomeric form in organic solvents. Sheppard and Geddes[11] observed that the spectrum of this dye in aqueous solutions of the cationic soap, cetyl pyridinium chloride, is favorable to the "organic spectrum." This was explained on the basis of a partition of the dye between water and colloidal micelles with the dye in the latter environment showing the spectrum characteristic of its solutions in non-polar solvents. As indicated below, the change in spectrum in solutions of anionic soaps is far greater than that in solutions of cationic soaps as reported by Sheppard and Geddes.

Considerable evidence has been advanced for the existence of micelles in which a solubilized material is dissolved between the non-polar ends of detergent molecules.[12] It thus appears probable that pinacyanol chloride is likewise dissolved in such a hydrocarbon-like layer and that the concentration at which its absorption spectrum in soap solutions changes toward that typical of its solutions in organic solvents marks the critical concentration for the formation of micelles.

In Fig. 1 are plotted the absorption spectra at 25.8°C of 1×10^{-4} molar pinacyanol chloride solutions of varying concentration with respect to potassium laurate. The effects are extremely remarkable. With minute amounts of soap, the water bands at 5200A and 5500A disappear and a new band appears at about 4800A. At a potassium laurate concentration of 2.3×10^{-2} molar, this short wave-length band begins to diminish in intensity and simultaneously the intensity of absorption bands at 5700A and 6150A increases rapidly. These latter two bands are characteristic of pinacyanol chloride solutions in organic solvents. The change may be made more striking by plotting the extinction coefficients at the band maxima against the soap concentration. Following Sheppard's notation, the bands are designated as α, β, and γ in order of decreasing wave-length. The data are presented in Table I and plotted in Fig. 2. The abrupt change in spectra at a soap concentration of $2.3\text{–}2.4\times10^{-2}$ molar is clearly demonstrated in Fig. 2. Although no authentic value for the critical concentration of potassium laurate is reported in the literature, the value given above may be compared to those obtained for sodium laurate. By conductivity Ekwall[11b] reports 2.8×10^{-2} molar, while Long and Nutting[13] obtained a value of 2×10^{-2} molar by the surface tension-time effect on a buffered system. The

TABLE I. The intensity of band maxima at various soap concentrations for 1×10^{-4} molar pinacyanol chloride in potassium laurate solutions at 25.8°C.

Soap concentration (molar)	Extinction coefficient $\left(\frac{\log_{10}(I_0/I)}{\text{cm (mole/l)}}\right)$		
	$\alpha\times10^4$	$\beta\times10^4$	$\gamma\times10^4$
2.90×10^{-5}	2.63[b]	5.19	4.31
5.88×10^{-5}	2.33[b]	3.84	3.07[a]
1.22×10^{-4}	1.02[b]	1.28[b]	1.56
2.90×10^{-4}	1.03[b]	1.35[b]	1.99
1.74×10^{-3}	0.74[b]	1.27[b]	2.97
4.25×10^{-3}	0.31[b]	0.61[b]	4.27
1.262×10^{-2}	0.35[b]	0.69[b]	4.74
1.710×10^{-2}	0.65[b]	1.26[b]	4.16
1.930×10^{-2}	0.92	1.18[a]	3.89
2.153×10^{-2}	1.19	1.23[a]	4.76
2.225×10^{-2}	2.52	2.09	4.08
2.321×10^{-2}	3.27	2.50	4.72
2.350×10^{-2}	3.90	3.06	4.56
2.394×10^{-2}	5.61	3.94	1.87
2.436×10^{-2}	5.87	4.41	1.43[a]
2.478×10^{-2}	5.89	4.63	0.29[b]
4.154×10^{-2}	6.38	5.06	0.17[b]
2.088×10^{-1}	6.26	4.24	0.31[b]

[a] Step-out.
[b] No band but a wave-length of corresponding band maxima at other soap concentrations.

[11] S. E. Sheppard and A. L. Geddes, J. Chem. Phys. **13**, 63 (1945).

[12] This evidence is summarized and literature references given in W. D. Harkins, R. W. Mattoon, and M. L. Corrin, J. Am. Chem. Soc. **68**, 220 (1946) and W. D. Harkins, R. W. Mattoon, and M. L. Corrin, J. Colloid Science **1**, 105 (1946).

[13] G. C. Long and F. A. Nutting, J. Am. Chem. Soc. **63**, 84 (1941).

TABLE II. The intensity at band maxima at various soap concentrations for 1×10^{-5} molar pinacyanol chloride in potassium laurate solutions at 25.8°C.

Soap concentration (molar)	Extinction coefficient $\left(\frac{\log_{10}(I_0/I)}{\text{cm (mole/l)}}\right)$ $\alpha\times10^4$	$\beta\times10^4$	$\gamma\times10^4$
2.023×10^{-2}	2.58	2.86[b]	7.45
2.055×10^{-2}	3.04	3.04[b]	6.50
2.104×10^{-2}	4.07	3.65	6.27
2.146×10^{-2}	5.23	4.41	6.99
2.173×10^{-2}	7.72	5.53	3.75
2.202×10^{-2}	9.79	6.54	2.27[a]
2.285×10^{-2}	11.55	7.42	2.07[b]
2.402×10^{-2}	12.74	7.23	1.36[b]
2.809×10^{-2}	12.68	6.48	0.70[b]

[a] Step-out.
[b] No band but at wave-length of corresponding band maxima at other soap concentrations.

presence of buffering salts would, however, tend to render this value low. With 1×10^{-5} molar pinacyanol essentially the same results were obtained; the data are given in Table II.

The slightly lower critical concentration obtained with the lower dye concentration is probably caused by the increased sensitivity obtained in that the partition of the dye between the micelles and water tends to mask the "organic spectrum" when but little of the dye can enter the micelles.

Similar results are obtained with potassium myristate as indicated in Fig. 2 and Table III. In this case the critical concentration at 25.8°C and in the presence of 1×10^{-4} molar pinacyanol chloride is 6×10^{-3} molar. A value of 7.0×10^{-3} molar for sodium myristate has been reported by Ekwall.[1b]

With sodium cetyl sulfate it was found necessary to decrease the dye concentration to 1×10^{-5} molar in order to fix sharply the critical concentration. The value obtained, $3.6\text{–}5.2\times10^{-4}$ molar at 35.8°C (Fig. 3), compares favorably with that reported by Lottermoser and Puschel[4] of $4\text{–}6\times10^{-4}$ molar on the basis of conductivity and a value of 4×10^{-4} molar by Nutting, Long, and Harkins[7b] by surface tension-time measurements. The data are given in Table IV.

The critical concentration for potassium dehydroabietate at 25.8°C is $2.5\text{–}3.2\times10^{-2}$ molar. The spectral change with this soap is less sharp than in the case of the potassium soaps of the straight chain acids as indicated in Fig. 3 and Table V.

The behavior of potassium oleate and of

TABLE III. The intensity of band maxima at various soap concentrations for 1×10^{-4} molar pinacyanol chloride in potassium myristate solutions at 25.8°C.

Soap concentration (molar)	Extinction coefficient $\left(\frac{\log_{10}(I_0/I)}{\text{cm (mole/l)}}\right)$ $\alpha\times10^4$	$\beta\times10^4$	$\gamma\times10^4$
5.31×10^{-3}	0.96	1.13[b]	6.74
5.82×10^{-3}	1.62	1.63[a]	6.68
6.02×10^{-3}	1.66	1.85[b]	7.25
6.31×10^{-3}	4.21	3.80	3.70
6.65×10^{-3}	7.02	6.55	1.19[b]
1.048×10^{-2}	6.94	6.43	0.59[b]

[a] Step-out.
[b] No band but at wave-length of corresponding band maxima at other soap concentrations.

potassium dilinoleate prepared by the dimerization of linoleic acid differs from that of the soaps described above. With potassium oleate, *a new band appears at 5200–5400A* after the disappearance of the 4800A band. This band persists during the development of the 6250A band. The absorption spectra are given in Fig. 4, the intensities of the maxima at various soap concentrations in Fig. 5 and Table VI. The variation in the 5700A band is more or less masked because of the proximity of the broad 5400A band. In this instance it is difficult to assign a critical concentration, and a provisional value of $7\text{–}12\times10^{-4}$ molar corresponding to the point of rapid development of the long wave-length band has been taken. No value for the critical concentration of this soap is found in the literature, although Ekwall[1b] has determined the conductivity of its solutions. The development of colloidal micelles would seem, from the spectroscopic evidence, to occur over a wide concentration range.

With potassium dilinoleate at 25.8°C the

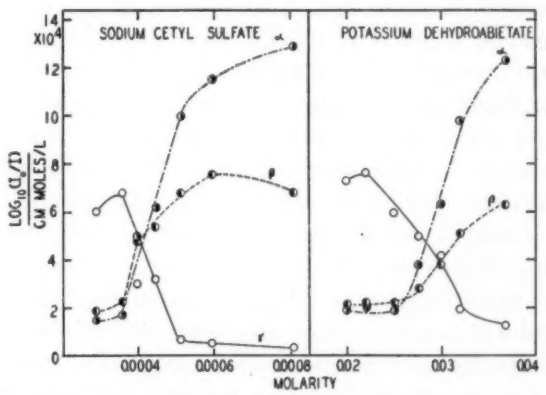

FIG. 3. Intensity of band maxima *versus* soap concentration for sodium cetyl sulfate and potassium dehydroabietate.

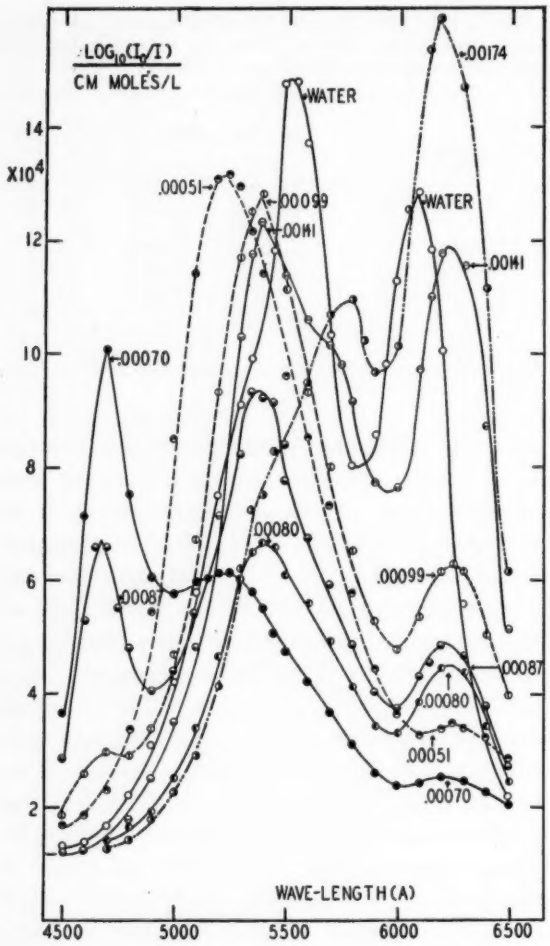

FIG. 4. Effect of varying potassium oleate concentration on the absorption spectra of pinacyanol chloride in aqueous solution.

4800A band fails to appear. The intensity of the band maximum at 5300A goes through a maximum at a soap concentration of 1.7×10^{-4} molar simultaneously with a constant intensity of the 6200A band. The 6200A band increases in intensity with soap concentration at soap concentrations greater than 2.5×10^{-4} molar. The data are given in Fig. 5 and Table VII. When the specific conductance of this material is plotted against the concentration, as suggested by Tartar, a break occurs at 3.0×10^{-4} molar as indicated in Fig. 6.

Since the color changes occurring at the critical concentration are very marked, it has been found possible to employ a visual rather than spectrophotometric method for such determinations. A soap solution of known concentration and containing pinacyanol chloride may be titrated with a solution of the dye in water and the critical concentration determined with a deviation of less than 1 percent of that determined spectroscopically. The titration technic affords an excellent means for the rapid and unambigu-

TABLE IV. The intensity at band maxima at various soap concentrations for 1×10^{-5} molar pinacyanol chloride in sodium cetyl sulfate solutions at 35.8°C.

Soap concentration (molar)	Extinction coefficient $\left(\frac{\log_{10}(I_0/I)}{\text{cm (mole/l)}}\right)$		
	$\alpha\times10^4$	$\beta\times10^4$	$\gamma\times10^4$
2.88×10^{-4}	1.52	1.90[a]	5.99
3.57×10^{-4}	1.75	2.23	6.80
3.97×10^{-4}	4.92	4.80	3.04
4.45×10^{-4}	6.18	5.35	3.21
5.13×10^{-4}	9.96	6.78	0.71[b]
5.94×10^{-4}	11.51	7.14	0.56[b]
8.11×10^{-4}	12.89	6.78	0.35[b]

[a] Step-out.
[b] No band but at wave-length of corresponding band maxima at other soap concentrations.

TABLE V. The intensity at band maxima at various soap concentrations for 1×10^{-5} molar pinacyanol chloride in potassium dehydroabietate solutions at 25.8°C.

Soap concentration (molar)	Extinction coefficient $\left(\frac{\log_{10}(I_0/I)}{\text{cm (mole/l)}}\right)$		
	$\alpha\times10^4$	$\beta\times10^4$	$\gamma\times10^4$
1.99×10^{-2}	1.92	2.12[b]	7.28
2.21×10^{-2}	2.17	2.20[b]	7.64
2.51×10^{-2}	1.88	2.20	5.95
2.76×10^{-2}	3.81	2.82	4.96
3.00×10^{-2}	6.34	3.83	4.18
3.19×10^{-2}	9.79	5.09	1.93[a]
3.68×10^{-2}	12.32	6.29	1.25[b]

[a] Step-out.
[b] No band but at wave-length of corresponding band maxima at other soap concentrations.

TABLE VI. The intensity at band maxima at various soap concentrations for 2×10^{-5} molar pinacyanol chloride in potassium oleate solutions at 25.8°C.

Soap concentration (molar)	Extinction coefficient $\left(\frac{\log_{10}(I_0/I)}{\text{cm (mole/l)}}\right)$			
	$\alpha\times10^4$	$\beta\times10^4$	$\omega\times10^4$	$\gamma\times10^4$
5.06×10^{-4}	3.47	7.33[b]	13.07	2.30[b]
5.93×10^{-4}	3.39	5.00[b]	12.33	2.27[b]
6.98×10^{-4}	2.53	3.66[b]	6.13	1.01[b]
8.02×10^{-4}	4.45	4.91[b]	6.65	1.41[b]
8.72×10^{-4}	4.86	5.90[b]	9.22	6.58
9.24×10^{-4}	5.40	7.24[b]	11.36	4.54
9.94×10^{-4}	6.30	8.02[b]	12.84	3.00
1.10×10^{-3}	8.00	9.32[b]	14.24	1.64[b]
1.26×10^{-3}	9.96	9.59[b]	13.10	1.55[b]
1.40×10^{-3}	5.88	5.07[a]	6.17	0.73[b]

[a] Step-out.
[b] No band but at wave-length of corresponding band maxima at other soap concentrations.

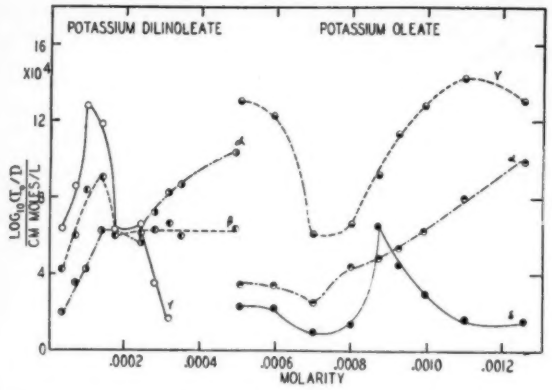

FIG. 5. Intensity of band maxima *versus* soap concentration for potassium oleate and dilinoleate.

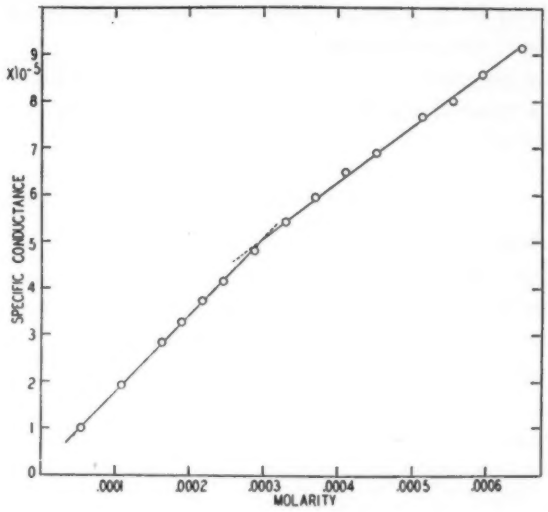

FIG. 6. Conductivity of dilute solutions of potassium dilinoleate.

ous investigation of the effect of salts and hydrocarbon additives on the critical concentrations of soaps. At present, the only method available for investigations on the effects of salts is a solubility method described by Tartar and Cadle.[14] The corrections to be applied to conductometric, freezing point, and similar methods are so uncertain in the presence of salts that these technics are of little value.

The critical concentrations of a few soaps are given in Table VIII.

EXPERIMENTAL

Materials.—Potassium laurate was prepared by saponification of a carefully fractionated sample of methyl laurate. The soap was twice recrystallized from ethanol and washed with acetone. It was dried in a vacuum.

Potassium myristate was obtained by the neutralization in hot ethanol with alcoholic potassium hydroxide of Eastman myristic acid which had been twice recrystallized from ethanol and once from acetone and which had been subjected to hydrogenation at 3 atmospheres over Adams platinum oxide catalyst. The soap was recrystallized twice from alcohol and washed with acetone.

Potassium oleate was prepared from a sample of oleic acid purified by Professor Reynolds of the University of Cincinnati. The acid, dissolved in hot alcohol, was neutralized with alcoholic potassium hydroxide and the soap recrystallized and carefully washed.

Potassium dehydroabietate was prepared in the same manner from a sample of dehydroabietic acid supplied by Dr. Shepherd of the University of Illinois.

The sodium cetyl sulfate was of the same lot employed by Nutting, Long, and Harkins in their investigation of surface tension-time effects. The potassium dilineoleate was supplied by the Eastern Regional Laboratories of the Department of Agriculture and labelled NRRL-1731-9.

Solutions.—All solutions were prepared by weight. The weighed sample of soap was dis-

TABLE VII. The intensity at band maxima at various soap concentrations for 1×10^{-5} molar pinacyanol chloride in potassium dilineoleate solutions at 25.8°C.

Soap concentration (molar)	Extinction coefficient $\left(\frac{\log_{10}(I_0/I)}{\text{cm (mole/l)}}\right)$		
	$\alpha\times10^4$	$\beta\times10^4$	$\omega\times10^4$
3.52×10^{-5}	1.96[a]	4.25[a]	6.40
7.04×10^{-5}	3.54	6.00[a]	8.57
9.85×10^{-5}	4.25	8.36[a]	12.80
1.41×10^{-4}	6.22	9.07[a]	11.88
1.76×10^{-4}	6.29	6.33	6.02
2.46×10^{-4}	5.65	6.61	6.14
2.81×10^{-4}	7.26	6.29	3.56[b]
3.17×10^{-4}	8.24	6.61	1.70[b]
3.52×10^{-4}	8.64	6.00	3.02[b]
4.93×10^{-4}	10.33	6.40	3.02[b]
5.63×10^{-4}	11.65	6.72	2.12[b]
7.04×10^{-4}	12.52	6.61	1.70[b]
1.06×10^{-3}	13.00	6.61	1.87[b]
1.76×10^{-3}	19.60	12.28	3.73[b]

[a] Step-out.
[b] No band but at wave-length of corresponding band maxima at other soap concentrations.

[14] H. V. Tartar and R. D. Cadle, J. Phys. Chem. **43**, 1173 (1939).

solved in a known amount of dye solution of proper concentration.

Apparatus.—The spectrophotometer employed was that described by Hogness, Zscheile, and Sidwell.[15]

DISCUSSION

Some evidence may be drawn from the spectroscopic behavior of pinacyanol chloride in soap solutions with respect to the nature of the transition occurring at the critical concentration. Hartley[16] has held that at concentrations below the critical concentration the soap exists in an unaggregated state, i.e., as a completely dissociated electrolyte; the conductometric studies of Scott and Tartar[17] support this view by indicating the sharpness of the break in the conductivity curves at the critical concentration and the conformity of the conductivity relations below the critical concentration with that typical of strong electrolytes. McBain,[18] however, has advanced the concept that an equilibrium exists at all times between aggregated and unaggregated soap and that even in extremely dilute solutions "ionic micelles" exist. According to this view, the critical concentration marks the point at which lamellar micelles are first formed.

It would seem, *a priori*, that the spectral behavior of pinacyanol chloride involving as it does the solubilizing action of lamellar micelles, could give no information concerning solutions in which no such micelles exist. However, the development of the short wave-length, 4800A, band has been observed in all soap solutions investigated with the exception of potassium dilinoleate. The reason for the appearance of this band is as yet unknown. This band does not appear, however, when salts, such as potassium chloride and sodium acetate, or bases, such as sodium hydroxide, are added to pinacyanol chloride solutions. The appearance of the 4800A band has been noted only in soap solutions; this suggests that soap solutions below the critical concentration differ somehow in nature from those of simple, short chain electrolytes.

TABLE VIII. Critical concentrations for the formation of soap micelles as determined by pinacyanol in a spectrophotometer.

Soap	Dye concentration	Temperature	Critical concentration
Potassium dilinoleate	$1\times10^{-5}M$	25.8°	2.5 $\times10^{-4}M$
Potassium dehydroabietate	$1\times10^{-5}M$	25.8°	2.5 – 3.2 $\times10^{-3}M$
Potassium oleate	$2\times10^{-5}M$	25.8°	7 –12 $\times10^{-4}M$
Potassium laurate	$1\times10^{-5}M$	25.8°	2.15– 2.20 $\times10^{-2}M$
Potassium laurate	$1\times10^{-4}M$	25.8°	2.3 – 2.4 $\times10^{-2}M$
Sodium cetyl sulfate	$1\times10^{-5}M$	35.8°	3.6 – 5.2 $\times10^{-4}M$
Potassium myristate	$1\times10^{-4}M$	25.8°	6.0 – 6.7 $\times10^{-3}M$

Another conclusion that may be drawn from the spectral data is that the lamellar, solubilizing micelles are not formed from only the soap present in excess of that required to give the critical concentration. It is improbable, for example, that 1×10^{-4} mole of potassium myristate could form micelles of sufficiently great solubilizing power to account for the pronounced change in spectra occurring on the addition of this amount of soap just at the critical concentration. Owing, however, to the fact that no conclusions can be drawn from the spectra with respect to the partitioning of the dye between the water and the non-polar layers in the micelles, no quantitative inferences may be made with respect to this phenomenon.

The micellar development of potassium myristate, potassium laurate, and sodium cetyl sulfate occurs over a short concentration range, as indicated by the fact that the long wave-length band increases rapidly in intensity. With potassium dehydroabietate this development is more gradual. The data for potassium oleate and potassium dilinoleate, while difficult of interpretation, indicate that with them the formation of lamellar micelles occurs over a wide concentration range.

The writers wish to thank Professor Thorfin R. Hogness for the use of his remarkable spectrophotometer.

[15] T. R. Hogness, F. P. Zscheile, Jr., and A. E. Sidwell, Jr., J. Phys. Chem. **41**, 379 (1937).
[16] G. S. Hartley, Kolloid Zeits. **88**, 22 (1939).
[17] A. B. Scott and H. V. Tartar, J. Am. Chem. Soc. **65**, 692 (1943).
[18] J. W. McBain, Nature **145**, 702 (1940).

Free Radical Determination in Biacetyl Photolysis

RALPH G. ASCAH,[1] MILTON BURTON,[2] JOHN E. RICCI, AND THOMAS W. DAVIS
Department of Chemistry, New York University, New York, New York

(Received March 29, 1946)

Biacetyl vapors have been decomposed by radiation of wave-length 2537A in a flow system. The total amount of decomposition was determined by collection and analysis of the gaseous products. The amount of methyl radical formed was determined by allowing the products to pass over and react with lead mirrors. The amount of lead transported establishes the maximum quantity of methyl formed assuming a ratio of CH_3 to Pb of 4:1. The data show that approximately one methyl group is released for every two or three molecules of carbon monoxide in the products and consequently that about half of the total reaction proceeds without the primary formation of free radicals. A Spence and Wild type of reaction scheme will explain both the analytical data and observations on fluorescence.

THE formation of biacetyl in the products of acetone photolysis has been taken as indicating the intermediate formation of acetyl radicals.[3] Some confirmation of this conclusion is to be found in observations using mirrors.[4] The non-appearance of biacetyl when the walls of the reaction system are kept at temperatures above 60° has been taken as evidence that acetyl radicals are unstable at higher temperatures.[5] The instability of acetyl radicals has been investigated by mirror methods;[6] it is found that the half-life of radicals from acetone decomposition is greater at 45° than at 100°. The reason assigned is that the acetyl radicals decompose according to the equation

$$CH_3CO \rightarrow CH_3 + CO, \qquad (1)$$

the reaction being slower at 45° than the disappearance of methyl radicals. The effect of (1) is constantly to renew the supply of methyl radicals as long as acetyl radicals remain. At 100°, on the other hand, reaction (1) is so fast that the gas stream carries only methyl radicals and without a supplementary source of additional radicals, the measured half-life is accordingly less than at 45°.

Since it would be desirable to have independent measurements of the rate of reaction (1), an attempt at such a measurement was made in connection with the study of the photo-chemical decomposition of biacetyl as a source of acetyl radicals, using the lead mirror technique. The plan was to remove all methyl radicals by contact with lead at one point, and then to pick up and count, by means of a second lead mirror further downstream, the new methyl radicals formed by acetyl radical decomposition in the intermediate region. It was further intended that through the use of different temperatures in this intervening zone, a variation in the rate of reaction (1) could be effected, whereupon an experimental energy of activation might be determined.

Actually this project proved impossible of accomplishment with lead as the agent for detecting the methyl radicals because the mirrors became insensitive when used at ordinary temperatures, and to maintain their sensitivity the mirrors had to be kept at 100°. At this temperature, the acetyl radicals decompose and the experiments give information only on the total radical content of the gas, that is, methyl plus all the acetyl radicals without distinguishing the kinds. Nonetheless the experiments were continued because they shed light not on the behavior of the radicals after they were released but rather on the nature of the original decomposition itself. If the initial reaction proceeds wholly to give free radicals (whether methyl or acetyl makes no difference when the mirrors are kept at 100°), the metal deposits should count one methyl radical for each molecule of carbon

[1] Present address: Canadian Industries, McMasterville, Quebec, Canada.
[2] Present address: Department of Chemistry, University of Notre Dame, Notre Dame, Indiana.
[3] M. Barak and D. W. G. Style, Nature **135**, 307 (1935).
[4] H. H. Glazebrook and T. G. Pearson, J. Chem. Soc. 567 (1937).
[5] R. Spence and W. Wild, Nature **138**, 206 (1936).
[6] M. H. Feldman, J. E. Ricci, and M. Burton, J. Chem. Phys. **10**, 618 (1942).

TABLE I. Vapor pressures of biacetyl.

Temperature °C	−13	0	10	15	21	26	30
Pressure mm	5.2	12	21	28	39	45	67

monoxide formed. It is on this investigation that we report in the present paper.

EXPERIMENTAL

Apparatus and Procedure

The experimental set-up resembles closely that used in earlier investigations in this laboratory.[7,8] The procedure consisted of passing biacetyl vapor, drawn from a reservoir of the liquid, through a quartz tube 13 cm of which was illuminated by the radiation from a low pressure spiral mercury resonance lamp surrounding the tube. The lamp was operated on a 5000-v transformer, the primary current of which was maintained at 6.4 amp. from a 110-v circuit. The lamp gives light principally of wave-length 2537A. The gases leaving the illuminated region were allowed to flow over lead mirrors and the products resulting from this procedure were trapped and subsequently examined for their content of volatile lead compounds and for other gaseous constituents. As a rule, the experiments were run in two successive parts, without lapse of time between. Provision was made for collecting the gaseous products during only one of the two periods but lead was determined for both. This procedure not only allowed duplicate determination of lead but permitted a verification of the undiminished reactivity of the mirror. Any poisoning of the mirror during the experiment would be revealed by disagreement in the amounts of lead recovered during the two periods. In all experiments, the temperature of the illuminated zone was kept at 100°–105° but the tubing between the reaction zone and the mirror, when the two were not adjoining, was at room temperature.

Mirrors

The method of preparation of the mirrors has been described earlier.[6,8] The sharpening of the mirrors, and the clean-up of lead downstream were done with acetone, however, rather than with biacetyl. The acetone was supplied, of course, from a storage bulb separate from the biacetyl. Such use of acetone avoided deposition of non-volatile decomposition or polymerization products with consequent deactivation of the metal deposits. Furthermore, the availability of the acetone made possible a convenient testing of the effect of biacetyl on the mirror. The sharpening of the leading edge of the mirrors was especially necessary when the metal deposit was close to the illuminated zone because the gradient of free radical concentration in this region is high. Slight variations in the position of the mirror, therefore, would have a large effect on the amount of lead picked up. All mirrors were 3.0 cm or more in length, a length found sufficient to give full lead recovery. After a mirror was laid down and sharpened, the system was thoroughly pumped out to remove residual acetone vapors before the mirror was put to use. A new mirror was prepared for each experiment.

It was observed rather early in the course of the present work that the photolysis products of biacetyl desensitize mirrors kept at room temperature. The loss of sensitivity was shown by a decrease in the amount of lead picked up during a standard experiment with acetone. Similar poisoning by acetaldehyde and propionaldehyde has been attributed to polymer formation.[9] The notion that the poisoning of mirrors is caused by precipitation thereon of some slightly volatile material is supported by certain preliminary experiments. It was observed that in two successive runs with the same mirror at room temperature, the lead pick-up was reproducible if the apparatus was thoroughly pumped out between runs. On the other hand, the lead pick-up was much less for a continuous ten-minute run than twice that for a five-minute run. With the mirrors at 100°, the desensitization largely disappears; consequently, in all the experiments reported here the mirrors were kept at 100° by heating with steam.

[7] L. May, H. A. Taylor, and M. Burton, J. Am. Chem. Soc. **63**, 249 (1941).

[8] M. H. Feldman, M. Burton, J. E. Ricci, and T. W. Davis, J. Chem. Phys. **13**, 440 (1945).

[9] T. G. Pearson and R. H. Purcell, J. Chem. Soc. 1151 (1935).

Lead Analysis

The determination of lead was accomplished essentially by the procedure already described in the modified end-point technique.[6,8] With known samples of lead nitrate and lead tetramethyl, containing 20 to 50 μg of lead, the accuracy of the determination was about 0.5 μg.

Gas Analysis

The gaseous products of the reaction were separated into two fractions, one consisting of gases volatile at liquid nitrogen temperatures, and the other of gases volatile at $-131°$ but not volatile at $-196°$C. The analyses were carried out in a semi-micro apparatus.[10] The gas volatile at $-196°$ is largely carbon monoxide as shown by the behavior over heated copper oxide and alkali. The remainder was shown by combustion with oxygen to be ethane. The material volatile at $-131°$ was found on combustion to behave exactly like a known sample of ethane and is reported therefore as ethane.

Materials

The biacetyl was a commercial preparation carefully fractionated, the portion boiling from 88.7 to 89.1°C being retained. The refractive index at 18.5°, namely 1.3930, checks closely the literature value. The biacetyl was stored at dry-ice temperatures and was carefully shielded from light. The vapor pressure of the substance was determined in the temperature range, $-13°$ to $+30°$. The measurements were made by immersing the storage bulb of biacetyl in constant temperature baths and observing on a mercury manometer the pressure developed by the vapor. The data are recorded in Table I.

The plot of log p *vs.* $1/T$ is quite linear and the heat of evaporation calculated therefrom is 109 cal. g^{-1}.

RESULTS

Data on the photolysis of biacetyl in the absence of a lead mirror appear in Table I .

The ratio of CO to C_2H_6 should be 2.0 If the sole products of decomposition are COi and C_2H_6. The average value of 2.2 suggests the formation of products more highly methylated than the starting substance. Several possibilities will be considered in the discussion below. A trend in the absolute amounts of carbon monoxide produced is without theoretical significance. It was noted that the figures for the amount of carbon monoxide produced per unit of time decreased with continued use of the apparatus. This trend is probably a consequence of decreased light input which in turn was caused by the repeated heating of the tube during the preparation of the mirrors. The quartz tube, it was noted, became visibly darker during the course of the experiments and no doubt this affected the transparency to ultraviolet.

TABLE II. Products of biacetyl photolysis. $\lambda = 2537$A; $t = 105$–110°C.

Expt. No.	Inlet flow pressure, mm	Time, min.	Gaseous products: Liq. nitrogen fraction: Total vol.[a]	Liq. nitrogen fraction: CO vol.	Liq. nitrogen fraction: Vol. of residue	−131°C fraction, vol.	Rate of production of CO[b]	Ratio CO/C_2H_6
23	3.6	5	13.50	12.70	0.82	4.83	2.54	2.2
24	3.6	5	12.90	12.70	0.21	5.31	2.54	2.3
25	3.6	10	25.4	24.9	0.47	11.05	2.49	2.2
26	3.6	10	25.7	24.9	0.75	—	2.49	—
76	3.6	5	8.51	—	—	—	(1.70)	—
77	3.6	5	8.21	—	—	—	(1.64)	—
89	3.6	5	6.85	—	—	3.13	(1.37)	<2.2
90	2.1	5	5.26	—	—	2.42	(1.05)	<2.2
93	2.1	5	5.35	5.11	0.24	2.36	(1.02)	2.0
94	1.6	10	6.97	6.65	0.32	2.78	(0.67)	2.1
							Av.:	<2.2

[a] All volumes are in units of 10^{-2} ml at S.T.P.
[b] Units of 10^{-2} ml/min.

Data from runs with mirrors at "zero" distance, that is to say, immediately adjacent to the region of illumination, appear in Table III. In preparing this table, it is assumed that the only reaction proceeding at the lead surface is $Pb + 4CH_3 \rightarrow Pb(CH_3)_4$. Each microgram of lead, therefore, is equivalent to 4.335×10^{-4} ml of gaseous CH_3 at S.T.P. or to one-half of this amount of ethane. The symbol ΣC_2H_6 is defined as a sum, *viz.*,

$$\Sigma C_2H_6 = C_2H_6 + \tfrac{1}{2}CH_3.$$

It is the total volume of ethane to be expected if all the methyl radicals were to combine to give ethane. The ratio $CO/\Sigma C_2H_6$ in experiments with mirrors replaces the ratio CO/C_2H_6 in experiments without mirrors as a kind of material-balance for the reaction. The expected

[10] K. W. Saunders and H. A. Taylor, J. Chem. Phys. 9, 616 (1941).

TABLE III. Products from biacetyl photolysis with mirrors at zero distance.

Expt. No.	Inlet pressure, mm	Time, min.	Pb found, μg	CH_3 (vol.)[a] equivalent to Pb	Gases (vol.)[a] CO	Gases (vol.)[a] C_2H_6	CO production rate[b]	CO/CH_3	Ratios CO/C_2H_6	$CO/\Sigma C_2H_6$
69	3.6	5.0	41							
		2.5	21							
74	3.6	2.5	23							
		5.0	42	1.82	8.45		1.69	4.6		
75	3.6	2.5	17							
		5.0	40	1.73	8.45		1.69	4.9		
83	3.6	2.5	22							
		5.0	47	2.04	7.92	3.43	1.58	3.9	2.3	1.8
86	3.6	5.0	33							
		5.0	43	1.86	7.69	2.84	1.54	4.1	2.7	2.0
87	3.6	5.0	40							
		5.0	44		7.27	2.72	1.45	3.8	2.7	2.0
										Av. 1.9
71	2.1	5.0	43							
		2.5	21							
79	2.1	2.5	15							
		5.0	30	1.30	6.45		1.29	5.0		
80	2.1	2.5	14							
		5.0	33	1.43	6.33	2.42	1.27	4.4	2.6	2.0
81	2.1	2.5	14							
		5.0	32	1.39	6.33		1.27	4.6		
82	2.1	2.5	22							
		5.0	34	1.47	6.26	2.42	1.25	4.3	2.6	2.0
										Av. 2.0
78	1.6	2.5	8							
		5.0	19	0.82	4.61		0.92	5.6		
84	1.6	5.0	10	0.43	4.08	1.42	0.82	9.4	2.9	2.5
85	1.6	10.0	26							
		10.0	30	1.30	7.69	2.72	0.77	5.9	2.8	2.3
88	1.6	10.0	41							
		10.0	42	1.82	7.04	2.42	0.70	3.9	2.9	2.1
										Av. 2.3

[a] In 10^{-2} ml at S.T.P.
[b] In 10^{-2} ml/min.

value is 2.0. The average value observed is about 2.1 with a few scattered results as high as 2.5 or as low as 1.8. There is no trend in the ratios deviating considerably from the average.

Correction for Radical Disappearance

Not all the radicals formed in the photolysis reach the mirrors even when the mirrors are immediately adjacent to the irradiated zone because some of the radicals disappear while traveling past the lamp on their way to the mirror. To determine the proportion of radicals thus escaping detection as lead tetramethyl, it is necessary to know the half-life of the radicals and the time taken to reach the mirrors. The time of transport was determined by weighing the amount of biacetyl flowing in a fixed time with various inlet pressures. The measurements indicated an initial velocity of 1380 cm sec.$^{-1}$ when the inlet pressure was 2.1 mm. The formula of Paneth and Lautsch may be used to convert distance of flow into time.[11] This formula corrects for the change in velocity due to change in pressure as the gas flows through the tube.

The half-life of the methyl radicals was established by measuring lead recovery with mirrors at different distances from the region where the radicals are formed. The half-life was found to be 2.5×10^{-3} sec., a figure which may be compared with 8×10^{-3} sec. and 4.8×10^{-3} sec. for the half-lives of methyls from acetone photolysis at streaming velocities of 3000 cm sec.$^{-1}$ and 1800 cm sec.$^{-1}$, respectively.[6,7] These values point to a possible dependence of half-life on rate of gas flow. Since the same type of apparatus of nearly identical dimensions was used in all three investigations, the differences in half-lives cannot be attributed to differences in geometry or differences in general procedure. The data on which the half-life is based in the present study appear in Table IV and are plotted in Fig. 1.

If no allowance is made for a concentration gradient over a given cross section of the reaction tube, a first-order disappearance of methyl radicals should lead to a straight-line plot of log γ *vs.* z where z is the time of transport and γ is the quantity of alkylated lead recovered per unit amount of carbon monoxide. The experimental data when plotted in this way do fall on a nearly straight line. But a plot of $(\gamma)^{\frac{1}{2}}$ *vs.* z is also nearly linear as required for a three-halves order reaction. The data, therefore, do not cover a sufficient range to allow a decision as to whether the disappearance is first or three halves order. Both possibilities are considered in further calculations.

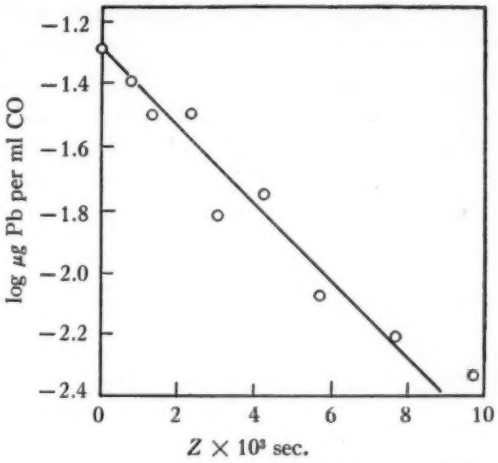

FIG. 1. Plot of first-order disappearance of methyl radicals outside the illuminated zone.

The calculation of the quantity of free radicals disappearing within the illuminated zone is made by the method already described for the photolytic decomposition of acetone.[8] The rate of change of methyl in the illuminated region is given by the expression

$$\frac{d[CH_3]}{dz}=k_1-k_2[CH_3]^n.$$

k_1, the rate of production of CH_3, is assumed constant for fixed conditions of T, P, and illumination (valid if the percentage of decomposition of biacetyl is very small). k_2 is the disappearance rate constant; its value, depending on the order assumed, i.e., n, is estimated from the half-life experiments.

Integration gives k_1 in terms of k_2, n, $[CH_3]$ and z, or $k_1=f(k_2, n, [CH_3], z)$; the total amount of CH_3 produced is then z_0k_1 or $z_0f(k_2, n, [CH_3], z)$, where z_0 is the time of travel through the illuminated zone. The introduction therefore of the specific values of $[CH_3]_0$ and z_0, ($[CH_3]_0$ being the amount of CH_3 equivalent to the lead picked up per unit time at z_0, that is, as the gases leave the illuminated zone), gives z_0k_1, or the total production of CH_3 per unit time, for any given value of n and hence of k_2; and z_0k_1 may then be compared with the amount of CO produced per minute, as the final significant ratio. On the

[11] F. Paneth and W. Lautsch, Ber. **64**, 2708 (1931).

TABLE IV. Rate of disappearance of methyl radicals from a gas stream at room temperature.

Expt. No.	Inlet pressure, mm	Duration of expt., min.	Mirror distance, cm	Time to reach mirror, ms.	Pb found, μg	CH_3 (vol.)[a] equivalent to Pb	Gas (vol.)[a] CO	Gas (vol.)[a] C_2H_6	$CO/\Sigma C_2H_6$
100	2.1	5	1.8	0.81	20				
		5			22	0.95	5.44	2.07	2.1
99	2.1	5	3.0	1.35	16				
		5			17	0.74	5.50	2.30	2.1
104	2.1	5	5.4	2.38	14				
		10			34	1.47	10.51	4.14	2.2
98	2.1	5	7.0	3.05	9				
		5			9	0.39	5.86	2.54	2.1
103	2.1	5	10.0	4.26	8				
		10			20	0.87	11.40	4.55	2.3
97	2.1	5	13.8	5.70	5				
		5			5	0.22	5.97	2.60	2.2
101	2.1	15	19.5	7.70	12.5				
		15			10.5	0.45	17.5	6.74	2.5
102	2.1	15	26.0	9.70	8.2				
		15			7.6	0.33	16.1	7.15	2.2
									Av. 2.2

[a] In 10^{-2} ml at S.T.P.

assumption that $n=1$, we find 0.42 ml of CH_3 produced per ml of CO. With $n=\frac{3}{2}$, we calculate 0.55 ml of CH_3 per ml of CO. These results refer to decomposition at 2.1 mm pressure of biacetyl. The corresponding figures, with $n=1$, and assuming k_2 independent of pressure (because data on half-lives were secured at the one pressure only), are 0.37 and 0.39 ml of CH_3 per ml of CO at 1.6 mm and 3.6-mm pressure, respectively. The "corrected" figures for total CH_3 production therefore are about double the uncorrected values.

The free radical disappearance in the illuminated zone is calculated as if this zone were at room temperature. This procedure leads to a maximum calculation of free radical production because the rate of decay of free radicals is less at higher temperatures than at low. That some of the radicals disappear in the gas phase as well as at the wall is possible but the experimental k_2 values do not distinguish between the processes. Use of the experimental k_2's includes allowance for both reactions.

While the over-all precision of the results is low, refinements in the calculations resulting from consideration of temperature gradients along the reaction tube and possible formation of $Pb_2(CH_3)_6$, etc., would lead to smaller calculated free radical production. The ratio of reaction proceeding by rearrangement to total reaction may be regarded, therefore, as a minimum value.

DISCUSSION

To be useful in interpreting the course of the reaction, the lead transported in these experiments must represent all or a known fraction of the methyl radicals produced. The experiments of Paneth and his co-workers show that probably all the methyl radicals reaching a film of lead are converted to lead tetramethyl.[12] A fuller discussion of the possibilities appears in an earlier paper,[8] and the arguments there presented apply equally well here. The weight of

[12] F. Paneth, W. Hofeditz, and A. Wunsch, J. Chem. Soc. 372 (1935).

evidence indicates that all the radicals coming to the mirrors are converted to volatile lead alkyls and probably to lead tetramethyl. On the basis of this statement, the data of this paper establish the fact that a very appreciable fraction of the biacetyl photolysis proceeds by a direct rearrangement into stable products. If the photolysis were wholly a process giving free radicals, 2.31 mg of Pb, equivalent to 1 ml of CH_3, should be recovered for every ml of CO produced. Actually the amount of lead found was much smaller than this and, as shown earlier, the value is between 0.86 and 1.25 mg, corresponding to .37–.55 ml of CH_3. Half of the reaction, therefore, seems to involve no free radicals at all.

The same situation is encountered in acetone photolysis.[8] When acetone molecules absorb light of proper frequency, they either split rather quickly into free radicals or, as a result of collision with other molecules, are put into a metastable state from which they are removed by collisional deactivation or by fission into stable molecules. Such a scheme was originally suggested by Spence and Wild.[13] Bowen and Horton[14] have suggested a somewhat similar course is biacetyl photolysis, namely,

$$\mathrm{Ac_2}+h\nu\rightarrow\mathrm{Ac_2}^* \longrightarrow \mathrm{Ac_2}^{**} \longrightarrow \text{products}$$
$$\mathrm{Ac_2}^* \xrightarrow{\text{deactivation}} \mathrm{Ac_2} \longrightarrow \text{deactivation}$$

where Ac_2** may be a tautomeric form of biacetyl. Almy and Anderson[15] have proposed independently a corresponding mechanism to explain fluorescence phenomena in biacetyl, namely,

$$\mathrm{Ac_2}+h\nu \underset{\text{fluorescence}}{\rightleftharpoons} \mathrm{Ac_2}^* \rightleftharpoons \mathrm{Ac_2}^{**} \text{ (long lived)}.$$

A combination of these schemes will account for the data presented in this paper if we assume also that the formation of free radicals occurs from the initially excited state and that the decomposition of the metastable molecules gives stable products.

The lead mirror experiments, while showing that the photo-decomposition proceeds partly by way of free radicals and partly by ultimate molecule rearrangement, do not themselves establish the nature of the free radical intermediates. Bergmann and Samuel[16] have considered the photolysis of biacetyl theoretically and have concluded that at long wave-lengths, the important reaction is

$$\mathrm{Ac_2}\rightarrow \mathrm{CO}(^1\Sigma)+\mathrm{CH_3}+\mathrm{CH_3CO}. \quad (2)$$

Other possibilities in our experiments leading to free radicals are

$$\mathrm{Ac_2}^*\rightarrow \mathrm{CH_3CO}+\mathrm{CH_3CO} \quad (3)$$

and

$$\mathrm{Ac_2}^*\rightarrow \mathrm{CH_3}+\mathrm{CH_3COCO}, \quad (4)$$

followed at 100° by

$$\mathrm{CH_3COCO}\rightarrow \mathrm{CH_3CO}+\mathrm{CO} \quad (5)$$

and

$$\mathrm{CH_3CO}\rightarrow \mathrm{CH_3}+\mathrm{CO}. \quad (6)$$

The molecular rearrangement would presumably be a slower reaction, depending, as it must, on the matching of several phase relations. The rearrangement may give three stable products, namely, ethane, acetone, and carbon monoxide, thus,

$$\mathrm{Ac_2}^{**}\rightarrow \mathrm{CH_3COCH_3}+\mathrm{CO}, \quad (7)$$

$$\mathrm{Ac_2}^{**}\rightarrow \mathrm{C_2H_6}+2\mathrm{CO}. \quad (8)$$

These two reactions proceed simultaneously with the free radical splits.

The free radicals released in reactions (5) and (6) disappear ultimately by reaction with each other to give ethane and carbon monoxide. That they do not react with biacetyl molecules to cause cracking of the biacetyl is shown by the fact that the presence of a mirror has no effect on the total carbon monoxide production. The following reactions, therefore, have no large importance in our own experiments:

$$\mathrm{Ac_2}+\mathrm{CH_3}\rightarrow \mathrm{C_2H_6}+\mathrm{CH_3COCO}, \quad (9)$$

$$\mathrm{Ac_2}+\mathrm{CH_3}\rightarrow \mathrm{CH_3COCH_3}+\mathrm{CH_3CO}; \quad (10)$$

also,

$$\mathrm{Ac_2}+\mathrm{CH_3}\rightarrow \mathrm{CH_4}+\mathrm{CH_2COCOCH_3}. \quad (11)$$

Reaction (11) is eliminated because no methane appeared in the products; had as much as 1 or 2 percent been formed, it would have responded to our repeated test for it.

[13] R. Spence and W. Wild, J. Chem. Soc. 352 (1937); 590 (1941).

[14] E. J. Bowen and A. T. Horton, J. Chem. Soc. 1505 (1934).

[15] G. M. Almy and S. Anderson, J. Chem. Phys. **8**, 805 (1940).

[16] E. Bergmann and R. Samuel, J. Org. Chem. **6**, 1 (1941).

Operating at somewhat higher pressures and higher temperatures, Roof and Blacet[17] observed a very important amount of methane in biacetyl photolysis and indeed, except at 25°, found more methane than ethane. The proportion of methane reported by Roof and Blacet nearly matches that in the pyrolysis as observed by Rice and Walters.[18] Reaction (9) is regarded by Rice and Walters as unlikely on theoretical grounds for it means capture of an exposed negative group by a free radical.[19] The reaction

$$CH_3+CH_3CO\rightarrow C_2H_6+CO, \qquad (12)$$

while not objectionable theoretically, is not important in acetone photolysis under conditions similar to those in our experiments, and probably plays no important part in the photodecomposition of biacetyl.

While hydrogen, methyl, or acetyl groups seem not to be captured from biacetyl molecules by free methyl radicals, there is the possibility that methyl radicals condense with biacetyl to give some kind of complex, presumably, first a radical and then a polymer. Perhaps the deposition of such a product is the cause of the decay in mirror activity when biacetyl is decomposed.[20] At 100°, either the complex is unstable (like the acetyl radical itself) or it is sufficiently volatile not to deposit on the metal surface. While the data are not very precise some support for this view is to be found in the behavior of the CO/C_2H_6 ratios in presence and absence of mirrors.

Quantum yields in biacetyl decomposition have been measured by Roof and Blacet, who observed that the CO quantum yield rises to rather high values above 100°. A rough extrapolation of their curves would indicate a yield in the neighborhood of 2 under the conditions of our experiments. The question arises at once, of course, as to whether our present experiments are compatible with this figure. There is no way for the direct ultimate-molecule reaction to give yields in excess of unity. While "cracking" reactions, (9)–(11), may give rise to chains which would increase the quantum yields, they seem actually to be of minor importance under the conditions of our present experiments. A decomposition of biacetyl induced by "hot" radicals[21] or by photo-activated molecules in the metastable upper state will explain the observed quantum yields. The reaction sequence, therefore, may include reactions like

$$CH_3COCOCH_3 \xrightarrow{\text{induced by } M} C_2H_6+2CO, \qquad (13)$$

where M is a hot radical or an energy-rich photoactivated molecule. Reaction (13) is nearly thermoneutral so that one "M" may induce the decomposition of many biacetyl molecules. It may be noted that rough estimates of the free energy show biacetyl to be rather unstable with respect to ethane and carbon monoxide under ordinary conditions, so that reaction (13) could proceed "spontaneously."

A study of the effects of foreign gases in the photolysis of biacetyl may at first glance appear to contradict the present findings. Nitric oxide in large concentration, for example, completely inhibits the formation of ethane.[22] This means either that all the initial reaction gives methyls, all of which are removed by a very efficient combination with nitric oxide, or that the intermediate activated molecules, which would normally rearrange to give ethane, are converted by nitric oxide into other products. Actually no information is given by the nature of the products, in the presence of nitric oxide, concerning the relative importance of the two reaction paths.

Although the rate of flow of reactive vapors in the experiments reported in this paper was so slow that a considerable proportion of the methyl radicals was consumed before the vapors emerged from the lighted zone, there can be little doubt that some of the photoactivated biacetyl under ordinary conditions decomposes by direct rearrangement into stable products, a conclusion in keeping with observations on the fluorescence of biacetyl.

[17] J. G. Roof and F. E. Blacet, J. Am. Chem. Soc. **63**, 1126 (1941).
[18] F. O. Rice and W. D. Walters, J. Chem. Phys. **7**, 1015 (1939).
[19] Cf. F. O. Rice and E. Teller, J. Chem. Phys. **6**, 489 (1938).
[20] Cf. P. A. Leighton and F. E. Blacet J. Am. Chem. Soc. **54**, 3165 (1932).
[21] Cf. W. M. Garrison and M. Burton, J. Chem. Phys. **10**, 730 (1942).
[22] H. W. Anderson and G. K. Rollefson, J. Am. Chem. Soc. **63**, 816 (1941).

The Crystal Structure of Synthetic Boehmite

PAUL P. REICHERTZ AND W. JACQUE YOST
Magnolia Petroleum Company, Dallas, Texas

(Received April 19, 1946)

Crystal structure computations have been made for synthetic boehmite, the α-modification of aluminum oxide monohydrate, using the powder method. The experimental data were found to fit an orthorhombic lattice with constants $a_0=2.85_9$A, $b_0=12.2_4$A, and $c_0=3.69_1$A. The assignment of four AlO (OH) groups to this unit cell gives a calculated density of 3.06_3 g/cc. The observed density is 2.97_7 g/cc. The general space group extinctions were found to agree with those of D_{2h}^{17}. Generalized atomic coordinates were roughly determined by application of Pauling's coordination theory for ionic crystals and the determinations refined by the usual intensity computations. The parameter values selected were $u_{Al}=-0.334$, $u_{OI}=0.287$, $u_{OII}=0.067$. It is suggested that the inconsistencies which exist between the experimental and computed intensity data may be explained by the occurrence of a small quantity of γ–Al_2O_3 in the synthetic samples used. The value of 2.47 ± 0.07A obtained for the hydrogen bridge distance is discussed. This value is less than that observed for any previously determined structure.

I. INTRODUCTION

SINCE the first production and identification of synthetic boehmite by Böhm and Niclassen[1] in 1924, a considerable literature has appeared concerning its production in the laboratory and its relation to the other known hydrates of aluminum. Despite some doubts as to the existence of such a monohydrate,[2] it has been repeatedly confirmed that such a crystalline modification does exist[3,4] and the mineralogical counterpart of the synthetic material has been found in many bauxites.[5] The cumulative result of this work has demonstrated that the hydrated oxides of aluminum are isomorphous with those of iron and has resulted in structural determinations of all the hydrates of alumina except boehmite. The structural determination of boehmite has probably been delayed by the difficulty of obtaining adequate single crystals. Achenbach[6] and Goldsztaub[7] have stated, however, that the crystal is orthorhombic and Dana[8] mentions that the boehmite crystals found in the French bauxites are microscopic orthorhombic plates.

The structure of lepidocrocite, the hydrated oxide of iron isomorphous with boehmite, has been obtained by Ewing[9] using oscillation and rotation photographs of a naturally occuring single crystal. Since no single crystal of boehmite, either natural or synthetic, was available or procurable, the work reported here has confined itself to powder techniques. The approach is based on the known similarity of the powder photographs of lepidocrocite and boehmite[7] and on the previously determined structure of lepidocrocite. The space group assigned to boehmite was that assigned to lepidocrocite by Ewing[9] and generalized atomic coordinates were determined by application of Pauling's coordination theory for ionic crystals,[10] and refinements in their determination made by appropriate intensity computations.

II. EXPERIMENTAL

A. Manufacture of Boehmite

Two samples of well-crystallized boehmite (designated as *A* and *B*) were used in this work. Sample *A* was obtained by peptizing pure aluminum metal with formic acid. The precipitate which separated during this process was heated under water vapor pressure at 150 to 175 degrees

[1] J. Böhm and H. Niclassen, Zeits. f. anorg. Chemie **132**, 5 (1924).
[2] H. B. Weiser and W. O. Milligan, J. Phys. Chem. **36**, 3010 (1933).
[3] H. Lehl, J. Phys. Chem. **40**, 47 (1936).
[4] J. D. Edwards and M. Tosterud, J. Phys. Chem. **37**, 483 (1933).
[5] J. Böhm, Zeits. f. anorg. Chemie **149**, 203 (1925).
[6] H. Achenbach, Chem. Erde **6**, 307 (1931).
[7] S. Goldsztaub, Comptes rendus **193**, 533 (1931).
[8] E. S. Dana, *Textbook of Mineralogy* (John Wiley & Sons, 1932) fourth edition, p. 503.
[9] F. J. Ewing, J. Chem. Phys. **3**, 420 (1935).
[10] L. C. Pauling, J. Am. Chem. Soc. **51**, 1010 (1929).

FIG. 1. Synthetic AlO (OH). Sample *A*. (20,000 ×)

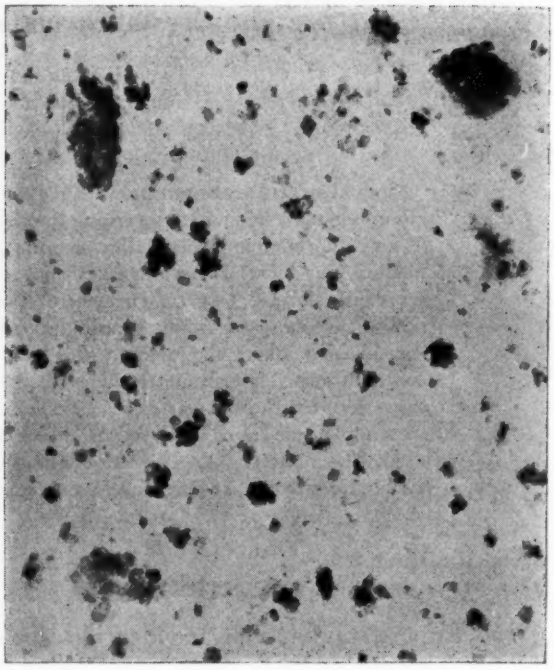

FIG. 2. Synthetic AlO (OH). Sample *B*. (20,000 ×)

C for four days, then dried at 100°C. Only a small amount of this sample was obtained. Sample *B* was prepared by peptizing pure metallic aluminum in 1 percent nitric acid at room temperature. The alumina trihydrate thus obtained was dried at 100°C. It was then placed in a glass lined bomb together with distilled water and heated for one week at 175°C. The contents were then dried at 105°C for 36 hours.

The two samples gave identical x-ray patterns which checked with published patterns for boehmite. Strong diffraction lines were obtained and no additional lines characteristic of the oxides or other hydrates of aluminum oxide could be observed. Computations from the half-widths of the stronger lines gave crystallite sizes in the neighborhood of 100A, for sample *B* and 60A for Sample *A*. For both Samples *A* and *B*, the innermost line was appreciably broader than any other on the pattern. Electron micrographs of the two samples indicate an apparent difference in habit despite the identity of the x-ray patterns. Figures 1 and 2 are reproductions of the micrographs of the two samples. The corresponding x-ray diffraction patterns recorded with Cu $K\alpha$ radiation are shown in Fig. 3. Sample *A* appears to consist of chains of discrete particles, the elements of the chains being insufficiently resolved to ascertain any characteristic shape or form. Their average diameter is in the neighborhood of 200A. Sample *B*, on the other hand, appears to consist of tabular particles, orthorhombic in character. They are apparently extremely thin, since the average particle is almost transparent to the electron beam. Their size varies from less than 100A to about 800A on a side.

The difference between the physical habits of the two crystallographically identical samples has not been explained. The rough agreement obtained between the values of particle size determined from the electron micrographs and those obtained from computation of x-ray line breadths does indicate that the particles observed are probably single crystallites or, at most, loose groupings of very few single crystals.

The density of Sample *B* was determined with a helium densitometer and found to be 2.97$_7$ g/cc. Fricke and Severin[11] quote a value of 3.014 g/cc

[11] R. Fricke and H. Severin, Zeits. f. anorg. Chemie **205**, 287 (1932).

while von Nieuwenburg and Pieters[12] give 3.06 g/cc.

The water content of Sample *B* was determined in the following manner. A sample was heated for 7 days at 115°C to remove the adsorbed water. A portion of this was then weighed, heated for 2 days at 500°C, and reweighed. Previous tests with numerous hydrated alumina samples indicated that the latter treatment was sufficient to convert the material to γ–Al_2O_3. For Sample *B*, the loss of weight was 15.0 percent, in perfect agreement with the theoretical water content of the monohydrate, $Al_2O_3 \cdot H_2O$. A second portion of the predried sample was ignited at approximately 1100°C and the resulting weight loss was 16.0 percent. The extra 1.0 percent loss may be caused by contaminants which volatilize at the higher temperatures or by water which remains adsorbed at 500°C.

All evidence, therefore, seems to indicate that the samples examined were boehmite.

B. Equipment

Electron micrographs were taken at an electronic magnification of 10,000 diameters and subsequently enlarged optically to a total magnification of 50,000 diameters. A type *B* RCA electron microscope was used for this work.

X-ray diffraction patterns were recorded with cylindrical powder cameras of diameter 14.32 cm. Both Mo $K\alpha$- and Cu $K\alpha$-radiations were employed and in all cases the radiation was monochromated by a quartz crystal. In general, the sample was contained in a parlodion capillary of diameter 0.45 mm. It is estimated that the precision of determination of Bragg angle, excluding absorption effects, is ±0.01°. This corresponds to an error of 0.001A at an interplanar spacing of 3.000A and to ±0.0005A at a spacing of 2.000A when copper radiation is used. Line densities were determined with a Leeds and Northrup microphotometer and Speedomax pen recorder.

TABLE I.

Present work	Goldsztaub
$a_0 = 2.85_9$A	2.85A
$b_0 = 12.2_4$A	11.8A
$c_0 = 3.69_1$A	3.78A

III. STRUCTURAL DETERMINATION

A. Unit Cell

The experimental data from the two samples (*A* and *B*) were found to fit an orthorhombic lattice, as suggested by the isomorphic character of lepidocrocite and boehmite. The lattice constants determined by us as compared with values reported by Goldsztaub[13] are shown in Table I.

The assignment of four AlO (OH) groups to our unit cell gives a density of 3.063 g/cc which is to be compared to the measured value of 2.97_7 g/cc.

Typical agreement between computed and experimental interplanar spacings is shown in Table II. A method of successive approximations was used to obtain lattice constants which yielded d_{theory} values agreeing most closely with d_{exp} values. The final step in this process consisted of fitting four d_{exp} values to their respective d_{theory} values as a correction for film shrinkage and similar camera errors. The agreement between the theoretical values and the average of measure-

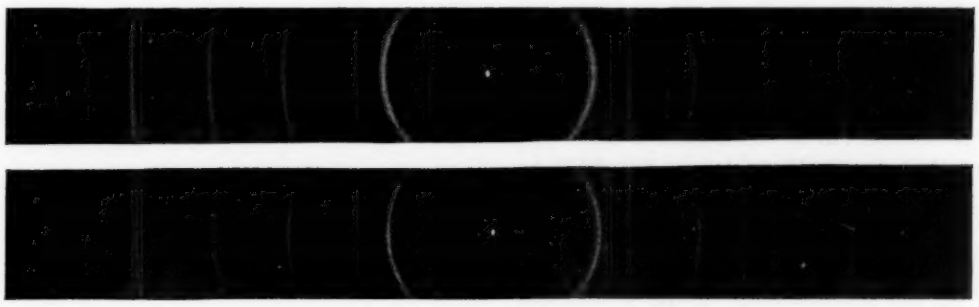

FIG. 3. Powder patterns of synthetic AlO (OH).

[12] C. J. von Nieuwenburg and H. A. J. Pieters, Rec. Trav. Chim. **48**, 27 (1929).
[13] S. Goldsztaub, Bull. Soc. franc. miner **59**, 348 (1936).

TABLE II. Sample *B*, Cu *Kα*-radiation.

(*hkl*)	d_{theory}	d_{exp}	d_1**
020	6.119	6.119*	6.132
021	3.160	3.160	3.153
130	2.341	2.341*	2.337
131	1.977	1.978	
002	1.845	1.845*	1.847
022	1.767	1.766	
151	1.661	1.659	1.654
080	1.530	1.523	
132	1.449	1.447	1.445
200	1.429	1.431	1.427
220	1.392	1.394	
171	1.383	1.379	1.385
152	1.310	1.307	1.304
202	1.130	1.131	

* Values set equal to d_{theory}.
** Average of measurements on 18 films of other synthetic boehmites. No film shrinkage corrections are included.

TABLE III. Atomic coordinate values.

Coordinate	Coordination value	Range studied Upper limit	Lower limit	Selected
u	−0.315	−0.340	−0.315	−0.334
u_1	+0.287	+0.280	+0.294	+0.287
u_2	+0.083	+0.063	+0.083	+0.067

ments on 18 other samples, all recorded and measured in a routine fashion, is gratifying also.

B. Space Group

The general extinctions observed for boehmite were the same as those observed for lepidocrocite by Ewing. No first-order reflections were found for $(k+l)$ odd and hence a lattice end-centered on (100) and based on Γ_0' is to be expected. If holohedral symmetry is assumed for boehmite, the space groups possible are limited to D_{2h}^{17} through D_{2h}^{22}. The existence of first-order prismatic reflections of the type (*hko*), h and k odd, eliminates D_{2h}^{18}, D_{2h}^{21}, and D_{2h}^{22}. Since reflections of the type (*okl*) with l odd are observed, D_{2h}^{20} is eliminated. D_{2h}^{19} permits all (*hol*). However, (*hol*) are observed only for h and l even. Therefore, D_{2h}^{19} is improbable. All of the absences observed are accounted for by D_{2h}^{17} and hence it is the best choice.

In order to avoid O–O distances of 1.85A or less, it is necessary that the eight oxygen atoms be placed on the intersections of the symmetry planes. Assuming that the aluminum atoms cannot be at the centers of symmetry, the generalized coordinates of the atoms are given by the following, in which the origin is taken at the center of symmetry:

4Al in 4(*c*) at 0, u, $\frac{1}{4}$; 0, $\bar{u}$, $\frac{3}{4}$; $\frac{1}{2}$, $u+\frac{1}{2}$, $\frac{1}{4}$; $\frac{1}{2}$, $\frac{1}{2}-u$, $\frac{3}{4}$
$4O_I$ in 4(*c*) at 0, u_1, $\frac{1}{4}$; etc.
$4O_{II}$ in 4(*c*) at 0, u_2, $\frac{1}{4}$; etc.

The generalized form of the crystal structure factor, F, is expressed by

$$F=\sum_j f_j \exp\left[2\pi i(hx_j+ky_j+lz_j)\right], \qquad (1)$$

where f_j are the atomic structure factors of the various atoms entering into the composition of the crystal. If the generalized coordinates for boehmite are substituted in (1), one obtains after simplification and reduction the following ex-

TABLE IV. Experimentally observable lines.

d	*hkl*	Rel. I Exp.	Rel. I Comp.	Order Exp.	Order Comp.
6.119	020	100	100	1	1
3.160	021	48	45	3	3
2.355	041	42	1.6	4	4
2.341	130		41.0		
1.977	131	4.1	0.0	11	17
1.859	150	52	13.2	2	2
1.845	002		36.0		
1.785	061	4.1	0.4	10	12
1.766	022		2.8		
1.660	151	10.6	13.8	7	6
1.538	112	*	0.0	14	10
1.530	080		5.3		
1.449	132		7.9	8	7
1.429	200	21.1	13.3	6	5
1.413	081		5.2		
1.392	220		1.2	13	16
1.383	171	9.0	1.7	12	13
1.368	062		0.9		
1.302	221	17.9	2.9	5	8
1.310	152		3.3		
1.206	023	*	2.0	16	15
1.178	082	*	1.8	15	14
1.171	260		0.6		
1.165	191		0.4		
1.162	0 10 1	*	4.0	17	11
1.160	172		0.5		
1.130	202	*	5.4	9	9

* Lines too weak for accurate integrated intensity measurements to be made.

pression:

$$F=16\cos^2(\pi/2)(k+l)\times[\textstyle\sum_j f_j\cos(\pi/2)(h-4u_jk)]^2. \quad (2)$$

Before applying this formula to intensity calculations, it was necessary to determine approximate values for the generalized coordinates. This was done by application of Pauling's coordination theory for ionic crystals and involved the following assumptions:

a. The structure is built up from Al-centered oxygen octahedra. Al–O distances are approximately 1.9A and O–O distances about 2.70A.

b. $O^=$ and $(OH)^-$ anions are shared between four and two octahedra, respectively. The cations are thus effectively neutralized by neighboring anions.

c. Shared edges between octahedra are contracted to 2.50A. Other edges are correspondingly lengthened. The octahedra are therefore distorted from a regular shape.

The orientation of the octahedra in the unit cell is suggested by the fact that the c_0 value of 3.691A is close to the value of 3.82A which is the length of the body diagonal of an undistorted octahedron. Correspondingly, the a_0 value of 2.859A can be most easily linked with the lengthened edge of an octahedron. This picture suggests a layer structure similar to that found for lepidocrocite. The a and c identity distances would be in the plane of the layer and correspond to the body diagonal and edge of an octahedron, respectively. The b identity distance would then be perpendicular to the layers with each layer very probably translated through a distance of $b/2$.

Carrying through the appropriate geometrical considerations given above, the following values were obtained for the generalized coordinates:

$$u=-0.315,\quad u_1=0.287,\quad u_2=0.083. \quad (3)$$

Intensity computations were made by application of the usual formula

$$I=N_p|F|^2F_p,$$

where

N_p—Number of planes in a given family,
$|F|$—Crystal structure factor (see Eq. (2)),
F_p—$(1+\cos^2 2\theta)/\sin\theta\sin 2\theta$.

The atomic structure factors chosen were those for the Hartree ion which have been published by James and Brindley.[14]

TABLE V. Computed lines not observed experimentally.

d	hkl	Computed rel. intensity 6.119A line = 100
3.060	040	1.7
2.784	110	0.0
2.222	111	0.0
2.040	060	2.3
1.580	042	0.5
1.492	170	1.1
1.295	240	0.2
1.228	190	0.2
1.224	0 10 0	0.4
1.222	241	0.0
1.125	113	0.0

During the progress of the computations, an attempt was made to include a correction due to sample absorption and also to apply the Debye-Waller temperature correction. Application of each of these corrections involves assumptions difficult to justify. However, each individual correction failed to improve the agreement between theoretical and experimental intensity values. In addition, it is easily demonstrated that the two corrections tend to nullify one another. Hence, they were not included in the final computations.

In the process of the computations, the generalized atomic coordinates were varied over a range sufficient to produce wide variations in the computed relative intensities. The ranges covered are given in Table III together with the values selected on the basis of best over-all agreement between experimental and computed intensities.

The limits of error on the final selection of generalized coordinates are difficult to estimate. However, the intensity values obtained would be in significant disagreement with experimental values if either upper or lower limit values or any combination of them given in Table III were used in the computations.

Computed and experimental results are presented in Table IV for the lines which were experimentally observed, while computed relative intensities for lines which were not experimentally observed are presented in Table V. The experimental relative intensities are those com-

[14] R. W. James and G. W. Brindley, Phil. Mag. **12**, 81 (1931).

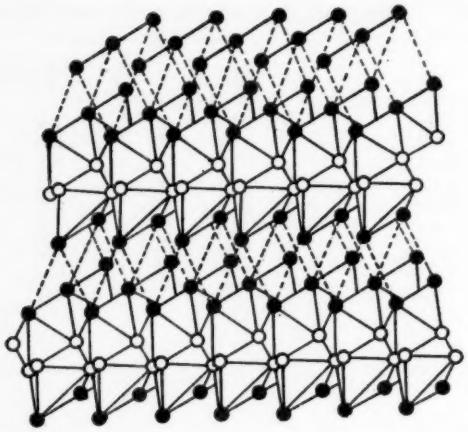

FIG. 4. Schematic diagram of boehmite structure. Dotted lines indicate (−OHOHO−) bonds. ○ = O_I positions; ● = O_{II} positions.

puted from the microphotometer trace of Sample *B*. Peak intensities were not used because of the wide differences in half-width from line to line. Rather, the traces of each line were replotted on a linear density scale using values obtained from the microphotometer trace. The areas under these replotted curves were then determined using a planimeter and were assumed to be a measure of the integrated intensity of each diffraction line. Since this procedure was valid only for relatively intense reflections, the experimental order of intensity was determined by an average of visual estimates of films of both Samples *A* and *B*.

IV. DISCUSSION

Considering the limitations and difficulties of the powder method of approach to problems of this nature, the agreement is gratifying. In particular, those reflections not experimentally observed should all have very weak intensities on the basis of these computations. However, particular features of the results as presented in Table IV seem to be in rather serious disagreement with experimental data. The (131) (221) and (152), and (171) and (220) reflections are much stronger in the experimental data than can be accounted for on the basis of the assigned structure. It is suggested that the interplanar spacings corresponding to these reflections are, within experimental error, the same as those of the stronger lines of γ–Al_2O_3. Since experimental intensities for these reflections are consistently higher than computed values, the discrepancy may be explained by postulating the occurrence of some γ–Al_2O_3 in the original boehmite. The other strong line of γ–Al_2O_3 which occurs at an interplanar spacing of 2.34A coincides in position with the fourth strongest line of boehmite as computed here and, hence, can have only very minor influence on the intensity of this line. This line of reasoning could be most easily justified by the usual single crystal type of analysis in which the crystalline purity of the sample would be beyond question.

A schematic diagram of the structure as calculated here is shown in Fig. 4. It is entirely similar in character to that found for lepidocrocite by Ewing[9] and hence need not be discussed here. The interatomic distances for this structure have been computed and are presented in Table VI. The marked distortion of the octahedra is to be noted. Also, the Al–O distances of 1.87, 2.06, and 1.93A exhibit an effect of Al–Al repulsion. Such an effect is not exhibited by lepidocrocite. These are to be compared with the corresponding distances of 1.99 and 1.85A found for corundum.[15] The smallest shared O–O distance of 2.50A is also to be compared with the value of 2.50A for corundum.

The hydrogen bonds which link the separate layers of oxygen octahedra are indicated by dotted lines. Such bonds are postulated on the basis of the short, unshared O–O distance between layers. This OHO distance of 2.47A is smaller than any similar distance previously known.[16] In particular, it is smaller than the corresponding hydrogen bridge distances for lepidocrocite (2.71A) and for diaspore (2.70A). This fact, corresponding as it does to increased bond energy, should result in a greater temperature stability of the boehmite crystallites over those of lepidocrocite and diaspore. Experimentally Sample *B* loses its water at approximately 450°C, while lepidocrocite undergoes a similar transition at 250°C[17] and diaspore at from 300 to 350°C.[18] The error in the determination of the hydrogen bridge distance in boehmite is

[15] L. C. Pauling, J. Am. Chem. Soc. **47**, 281 (1925).
[16] L. C. Pauling, *The Nature of the Chemical Bond* (Cornell University Press, New York, 1940), p. 311.
[17] W. H. Albrecht and O. Bandisch, J. Am. Chem. Soc. **54**, 943 (1932).
[18] W. H. Albrecht, Ber. **62B**, 1475 (1929).

difficult to estimate. It resides wholly in the error in determination of the parameter u_2. The best estimate (on the basis of intensity computations for various values of u_2) is that the OHO distance in boehmite is 2.47 ± 0.07A. Therefore even assuming maximum error, the hydrogen bridge distance for boehmite is only equal to the shortest previously known; namely, 2.54A for the tetragonal crystal KH_2PO_4.[16]

The OHO bonds are relatively weak in character and hence are easily sheared. This accounts for the apparent cleavage of boehmite and its existence in orthorhombic plates, such as are shown in the electron micrograph of Sample *B* (see Fig. 2). This factor may also account for the greater half-width of the (O2O) reflection which was consistently observed on a large number of preparations of synthetic boehmite. The weak hydrogen bonds would permit distortion of the "*b*" axis direction and this crystalline distortion could account for the varying values of line breadth observed from sample to sample and from diffraction line to diffraction line. Aside from the factor of distortion, the tendency for the crystal to occur in the form of thin crystalline plates would also account for the increased breadth of the (O2O) reflection.

TABLE VI. Interatomic distances in boehmite.

Atom	In the same octahedron	In other octahedra In same layer	In other octahedra In next layer
Al	$2O_{II}$ at 1.87A $2O_I$ at 2.06A $2O_I$ at 1.93A	2Al at 2.86A 2Al at 3.69A	
O_I	$2O_I$ at 2.86A $4O_{II}$ at 2.94A $4O_I$ at 2.50A $1O_{II}$ at 2.69A		
O_{II}	$2O_{II}$ at 2.86A $1O_I$ at 2.69A $4O_I$ at 2.94A		$2O_I$ at 4.66A $4O_{II}$ at 3.78A $2O_{II}$ at 2.47A

The authors wish to express their appreciation to Mr. J. M. Waite for assistance in the experimental x-ray work and to Mr. W. C. Skinner for the electron micrographs. We also wish to thank Dr. A. G. Oblad, Dr. H. T. Brown, and Mr. J. U. Messenger for the preparation of the boehmite and measurement of its density.

THE JOURNAL OF CHEMICAL PHYSICS VOLUME 14, NUMBER 8 AUGUST, 1946

Liquid Association and the Critical Temperature

FRANK BRESCIA
Chemistry Department, College of the City of New York, New York, New York

A THEORETICAL basis for a critical region instead of a critical point is furnished by Mayer who has calculated on a statistical mechanical basis[1] the general form of the pressure volume curve for a number of temperatures in the region of the critical temperature. The type of *P-V* diagram obtained for a pure liquid-saturated vapor system is such that two critical or characteristic temperatures, *Tm* and *Tc*, may exist. *Tm* is interpreted to correspond to the temperature at which the meniscus disappears and the surface tension becomes zero. This temperature is lower than the true critical temperature, *Tc*, the temperature at which the *P-V* curve has an inflection point for only one volume. At and above *Tc*, no differences exist between gas and liquid. Below *Tm*, a definite meniscus exists and the condensed phase has a surface tension. Between *Tm* and *Tc*, the *P-V* curve is horizontal over a finite volume and no surface tension exists. The magnitude of the temperature interval between *Tm* and *Tc* has not been theoretically calculated. This interval according to the Van der Waals equation is, of course, zero.

Since a liquid possesses a more definite structure (order) than a gas,[2] this structure may be regarded as persistent beyond *Tm* and not com-

[1] Mayer and Harrison, J. Chem. Phys. **6**, 87 (1938); Harrison and Mayer, *ibid.*, 101.

[2] Stewart, Chem. Rev. **6**, 483 (1929); Rev. Mod. Phys., **2** 116 (1930).

TABLE I. Critical temperatures determined from meniscus disappearance and from P-V isotherms.

System	Tm, stationary bomb	Tm, shaken bomb	Ref.	Tc	Ref.
Carbon dioxide	30.96°C		a	31.04°C	b
Ethane		32.23°C	c	32.27	d
Propane	96.85		e	96.81	d
Butane	152.2		f	152.01	d
Pentane	197.2		g	197	h
Ethylene		9.21	i	9.90	j
Propylene	91.4		k	91.4	k
	91.9		m	91.9	l
				96.4	n
Methyl ether	126.9		o	138	p
Ethyl ether	192.3		q	194.6	r
Methyl alcohol	240.6		q	not determined	
Ethyl alcohol	241.7		q		
	243.6		s	243.6	s
Water	374.2		t	380	u

[a] Kennedy, J. Am. Chem. Soc. **51**, 1360 (1929).
[b] Michaels, Blaisse, and Michaels, Proc. Roy. Soc. (London) **160A**, 358 (1937).
[c] See reference 3 in text.
[d] Beattie *et al.*, J. Am. Chem. Soc. **59**, 1589 (1937); **61**, 24, 924 (1939).
[e] Deschner and Brown, Ind. Eng. Chem. **32**, 836 (1940).
[f] Kay, Ind. Eng. Chem. **32**, 358 (1940).
[g] Young, J. Chem. Soc. (London) **71**, 446 (1897).
[h] Sage and Lacey, Ind. Eng. Chem. **34**, 730 (1942).
[i] See reference 4 in text.
[j] McIntosh and Maass, Can. J. Research **16B**, 289 (1938); Dacey, McIntosh, and Maass, *ibid.* **17B**, 206 (1939); McIntosh, Dacey, and Maass, *ibid.*, 241.
[k] Vaughan and Graves, Ind. Eng. Chem. **32**, 1252 (1940).
[l] Souders, Ind. Eng. Chem. **32**, 1252 (1940).
[m] Winkler and Maass, Can. J. Research **9**, 613 (1933).
[n] This temperature is the temperature at which the dielectric constant of the vapor equals that of the liquid. Marsden and Maass, Can. J. Research **13B**, 296 (1935).
[o] Tapp, Steacie and Maass, Can. J. Research **9**, 217 (1933).
[p] Approximate extrapolation from the measured (17) difference in densities of liquid and saturated vapor plotted as a function of temperature to the temperature at which density difference is zero.
[q] Fisher and Reichel, Mikrochemie V. Mikrochim. Acta **31**, 102 (1943).
[r] Schroer, Zeits. f. physik. Chemie. **140**, 381 (1929).
[s] Ramsay and Young, Phil. Trans. Roy. Soc. (London) **A177**, 123 (1886).
[t] Schroer, Zeits. f. physik. Chemie. **129**, 79 (1927); Callendar, Proc. Roy. Soc. (London) **A120**, 460 (1928); Khitarov and Ivanov, Zentr. Mineral. Geol. **1936A**, 46.
[u] This temperature is the temperature at which the density of the liquid equals that of its saturated vapor. Callendar, reference t.

pletely broken until Tc is reached, at which temperature the complete disorder characteristic of the gas state is finally attained. One would thus expect associated liquids to have larger intervals between Tm and Tc than the non-associated liquids. Data given in Table I show that carbon dioxide and the saturated lower hydrocarbons, typical unassociated liquids, possess, within the errors of the data, zero intervals or intervals too small for experimental detection. The more strongly associated lower ethers, alcohols, and water appear to have measurable intervals. A quantitative relationship between the degree of association and magnitude of the interval cannot be deduced, however, from the presently available data. Also, the physical significance of the Tm measurements made in stationary bombs is seriously questioned by the discovery that shaking the bomb vigorously has a profound effect not only upon the temperature at which the meniscus disappears but also increases greatly the precision with which such measurements may be made.[3] Shaking the bomb causes the meniscus to disappear at a lower temperature. Thus with ethylene, Tm is 9.50°C in a stationary bomb and 9.21°±0.015°C in a shaken bomb.[4] It is thus probable that the interval between Tm and Tc is small but also real for non-associated liquids.

Temperatures given as Tc in the table have been determined, unless otherwise noted in the references, from isotherms carefully measured through the critical region at small temperature intervals, as the temperature at which the tangent to the inflection point for an isotherm is horizontal.

[3] Mason, Naldrett, and Maass, Can. J. Research **18B**, 103 (1940).
[4] Naldrett and Maass, Can. J. Research **18B**, 118 (1940).

Letters to the Editor

THIS section will accept reports of new work, provided these are terse and contain few figures, and especially few halftone cuts. The Editorial Board will not hold itself responsible for opinions expressed by the correspondents. Contributions to this section should not exceed 600 words in length and must reach the office of the Managing Editor not later than the 15th of the month preceding that of the issue in which the letter is to appear. No proof will be sent to the authors. The usual publication charge ($3.00 per page) will not be made and no reprints will be furnished free.

Synthetic Patterson Maps

A. D. Booth
Birkbeck College, University of London, England
AND
Dorothy Wrinch
Department of Physics, Smith College, Northampton, Massachusetts
July 11, 1946

THE customary test of excellence of a structure is the agreement between the observed and the calculated values of the structure factors $F(h,k,l)$. The mere agreement is not, in itself, a *sufficient* condition for the validity of the postulated structure and it is, in general, only when considerations of chemical plausibility are added that the solution can be considered to be established. This has been shown, in the one-dimensional case, by Patterson[1] who remarks that, when the treatment is extended to three dimensions, the probability of more than one structure giving agreement, is negligible.

However satisfactory the numerical comparison, envisaged above, may be in the case of small molecules, it seems probable that, as the examination of large molecules proceeds, this computation of individual F values for each proposed structure will be difficult or impossible. The reasons for this are twofold: first, the mere labor of calculation will be severe and secondly, the finer details of atomic arrangement may be unknown. It is thus desirable that some method be made available whereby an assessment of the compatibility of any given molecular structure with the experimental observations may be made.

A solution of the problem lies in the construction of synthetic Patterson syntheses. The essence of the method is to determine the general lie of the Patterson map of the proposed structure, since it can be shown that, as the number of scattering centers increases, the appearance of the Patterson map becomes, for the most part, more and more dependent on the broad features of the structure. In order to test the plausibility of a proposed structure, a synthetic Patterson map may be constructed and compared with that obtained from the experimental data. If the two maps agree in sufficient detail, there is a high probability that the proposed structure is correct. Evidently any measure of agreement between the two is exactly equivalent to the same measure of agreement between the observed and calculated structure factors.

To make this technique capable of rapid application, it is desirable that the Patterson maps of various types of structure be constructed and recorded. A beginning has been made on this by Patterson[2] and by Wrinch[3] and it is hoped to publish a detailed study later.

A further application of the technique is possible, for if the phase angles of the structure factors be calculated from these functions, the standard process of Fourier refinement could be applied to the experimental data and finer details obtained.

One technical point in the construction of synthetic Patterson maps may be dealt with here. There is evidently no theoretical difficulty in constructing the three-dimensional Patterson map of the atomic centers of any proposed structure, though the procedure may be complicated and intricate when the number of atoms is large. The "sharpened" version of the Patterson synthesis[4] which has been found by Booth[5] to be of considerable utility may well prove inapplicable to large molecules since, whereas the number of available F values increases at most with the first power of the unit cell volume, the complexity in the Patterson map (i.e., the number of peaks) increases as the square of the same quantity. Thus it becomes questionable whether the sharpened Patterson, with only a limited number of terms, has any physical significance in such cases. It follows that we should study, not only the Patterson map of the atomic centers, but also the map of the electron density distribution of the atoms. The question therefore arises as to how to represent an atom in Patterson space. This question can be answered formally, whatever the electron density distribution may be, by the use of transforms,[6] since the Patterson distribution g_P corresponding to any distribution g is derivable from the transform of T^2, where T is the transform of g in reciprocal space. Thus for a radially symmetric distribution $g(r)$ for example, we have

$$NT(R)=4\pi\int_0^\infty r^2g(r)(\sin 2\pi rR/2\pi rR)dr,$$

where N is the total number of electrons in the distribution. It then follows that

$$g_P(r)=4\pi N^2\int_0^\infty R^2T^2(R)(\sin 2\pi rR/2\pi rR)dR.$$

It has been found by Booth[7] that the distributions of atoms obtained by synthesis are closely represented by expressions of the form

$$g(r)=A\exp(-pr^2).$$

To verify this, the cases of carbon, nitrogen, oxygen, chlorine, and sulphur were studied and the wide applicability of this expression was seen, even when a common p value is used for several different atomic types. The value suggested by the data is

$$p=4.69.$$

If we adopt this representation of the electron density distribution of an atom, the actual form of the distribu-

tion in Patterson space can be deduced. Thus with

$$g(r)=N(p/\pi)^{\frac{1}{2}}\exp(-pr^2),$$

$$T(R)=(p/\pi)^{\frac{1}{2}}\int_0^\infty r^2\,(\sin 2\pi rR/2\pi rR)dr\,\exp(-pr^2),$$

$$=2(p/\pi)^{\frac{1}{2}}\int_0^\infty \cos 2\pi rRdr\,\exp(-pr^2)=\exp(-PR^2),$$

where $Pp=\pi^2$. From the expression for $g_P(r)$ given above, it then follows that

$$g_P(r)=N^2(\pi/2P)^{\frac{1}{2}}\exp(-\tfrac{1}{2}pr^2)=N^2(p/2\pi)^{\frac{1}{2}}\exp(-\tfrac{1}{2}pr^2).$$

With the help of this expression, it is evidently possible to pass directly from the Patterson map of a pattern of atomic centers to the continuous map of the corresponding pattern of atoms, when the electron density distribution of the atoms is represented as described above.

[1] A. L. Patterson, Phys. Rev. **65**, 195 (1944).
[2] A. L. Patterson, Phys. Rev. **56**, 972 (1939).
[3] Dorothy Wrinch, "Fourier Transforms and Structure Factors," 1946. (Monograph 2 of the American Society for X-Ray and Electron Diffraction.)
[4] A. L. Patterson, Zeits. f. Krist. **90**, 517 (1935).
[5] A. D. Booth, unpublished.
[6] Dorothy Wrinch, Nature **157**, 226 (1946).
[7] A. D. Booth, Proc. Roy. Soc. in the press.

The O—O Bond Energy in Hydrogen Peroxide

GEORGE GLOCKLER AND GEORGE MATLACK*
State University of Iowa, Iowa City, Iowa
July 12, 1946

IN a recent paper, Skinner[1] amends the value for the O—O bond energy from 34.9 kcal. or 1.51 ev[2] to approximately 52 kcal. or 2.26 ev after assuming that the OH bond energy in H_2O_2 is not similar to the OH bond energy in H_2O, but is more nearly equal to the OH bond energy of the free radical (~100 kcal. or 4.35 ev). As a tentative explanation, a comparison of resonating structures of H_2O and H_2O_2 is offered. It appears to us, however, that the resonance structures discussed by Skinner can equally well be used to argue that the OH bond in hydrogen peroxide is more nearly like the similar bond in water than it is in the free hydroxyl radical, as can be seen from Fig. 1.

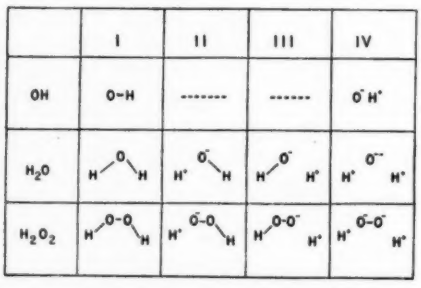

FIG. 1. Resonance structures involving hydroxyl groups.

TABLE I. Bond energies and interatomic distances of O—O bonds.

Substance	Bond energy (ev)	r_e(A)
$O_2(^3\Sigma_u^-)$	0.97[b]	1.60[a]
H_2O_2	1.51[b]	1.47[c]
O_3	3.06[d]	1.26[e]
$O_2(^1\Delta)$	4.11[b]	1.22[f]
$O_2(^1\Sigma_g^+)$	3.47[a]	1.223[a]
$O_2(^3\Sigma_g^-)$	5.08[g]	1.21[g]

[a] W. Jevons, *Band Spectra of Diatomic Molecules* (The University Press, Cambridge, England, 1932), p. 290.
[b] L. Pauling, *The Nature of the Chemical Bond* (Cornell University Press, Ithaca, New York, 1940), p. 53.
[c] Giguère and Schomaker, J. Am. Chem. Soc. **67**, 2025 (1945).
[d] Glockler and Matlack, J. Chem. Phys. (to be published).
[e] W. Shand and R. A. Spurr, J. Am. Chem. Soc. 65, 177 (1943).
[f] H. Sponer, *Molekülspektren* (Tabellen) (Verlagsbuchhandlung Julius Springer, Berlin, 1935), p. 16.
[g] G. Herzberg, *Molecular Spectra and Molecular Structure, I. Diatomic Molecules* (Prentice-Hall, Inc., New York, 1939).

Skinner states that, in his belief, the completely ionic structure of water (under IV) has no counterpart in the hydroxyl radical or in hydrogen peroxide. It would seem to us that there is quite an analogy between the purely ionic structures of the three molecules, whereas the OH radical has no counterpart to structures II and III in water and hydrogen peroxide. (Fig. 1.) The structures under IV (Fig. 1) are totally ionic configurations. Whether the double charge resides on one oxygen as in water or on the O—O complex as in hydrogen peroxide seems to us immaterial. The point is that in these models (IV) the structures have reached complete ionic character. On the other hand, figures II and III are only partially ionic in makeup, a situation which is impossible in hydroxyl radical. Following this analogy further, it would seem that the OH binding energy in hydrogen peroxide is more simi-

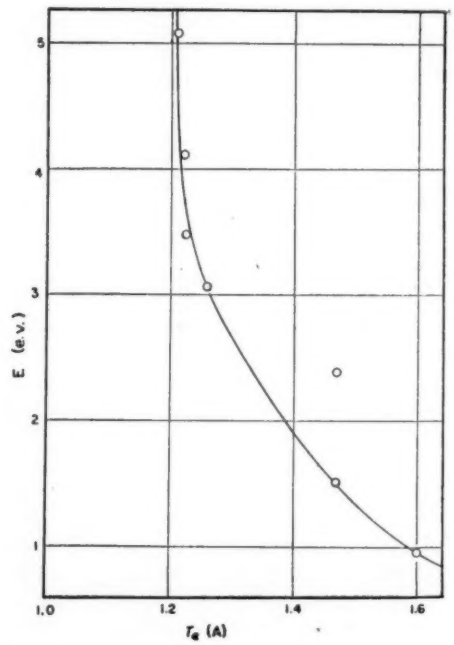

FIG. 2. Dissociation energies of oxygen bonds as a function of interatomic distances.

lar to that in water than to the free hydroxyl radical, as has been assumed by Pauling.[2]

Some empirical evidence is offered below which tends to support the lower value (1.51 ev) for the O−O bond in hydrogen peroxide. In connection with another problem, we have had occasion to calculate the O−O bond energies in several different molecules. We have made a comparison of the interatomic distances and bond energies as shown in Table I. These data are shown graphically in Fig. 2. It is seen that the O−O bond energy (2.37 ev) based on the assumption that the OH bond energy in H_2O_2 is more similar to the free hydroxyl radical does not fall on the curve obtained from the other structures containing O−O bonds. However, the O−O bond energy (1.51 ev) calculated on the basis that the OH bond in H_2O_2 is like the OH bond in water, fits very well into the curve, bond energy *vs.* interatomic distance. Hence the smaller value is to be preferred.

* A part of a thesis submitted in partial fulfillment of the requirements for the degree of Doctor of Philosophy, in the Department of Chemistry and Chemical Engineering, in the Graduate College of the State University of Iowa.

[1] Skinner, Trans. Faraday Soc. **41**, 645 (1945).
[2] Pauling, J. Am. Chem. Soc. **54**, 3570 (1932).

The Structure of Ozone

GEORGE GLOCKLER AND GEORGE MATLACK
Department of Chemistry and Chemical Engineering, State University of Iowa, Iowa City, Iowa
July 15, 1946

ADEL and Dennison[1] have recently re-examined the infra-red bands of ozone and have accepted the Hettner, Pohlman, and Schumacher assignment,[2] $\nu_1=2105$, $\nu_2=1043$, $\nu_3=710$ cm^{-1}, which results in an acute angle ($\alpha=34°$) isosceles triangle model, with $c_2=3.4$ and $c_1=0.6$ megadyne/cm, when a simple central force field is used. c_2 is the central field force constant between the oxygen atoms at the base of the isosceles triangle, c_1 is the force constant between the oxygen atoms at the apex and the base. They also estimated that the base internuclear distance is about 1A. At the present time there is a good deal of conflict regarding the correct fundamental frequencies and the structure of ozone. In this connection we wish to make the following remarks.

It seems difficult to believe that the base distance in ozone should be less than the interatomic distance in the oxygen molecule (1.21A). It would mean that the bond energy in the base pair of oxygen atoms is greater than the bond energy in the free molecule (see Fig. 1). We have calculated other isosceles models on the assumption that the sum of the bond energies must be 6.12 electron volts, obtained from the usual thermochemical calculation

$$3O \rightarrow O_3 \qquad \Delta E = 6.12 \text{ ev.}$$

Assuming that the base line is 1.21A (as in the oxygen molecule), the bond energy of the base pair in ozone is 5.08 ev (heat of dissociation of O_2). The bond between the apical oxygen and one of the base line atoms is then $\frac{1}{2}(6.12-5.08)=0.52$ ev, corresponding to 1.84A (see Fig. 1). The apical angle would then be 38°24′. Similarly, if 1.26A is taken to be the length of the base line, the energy curve yields 1.45A for the sides of the triangle and the apical angle is 51°30′.

If the base bond were only one angstrom in length, it would mean that electrons from the third incoming oxygen

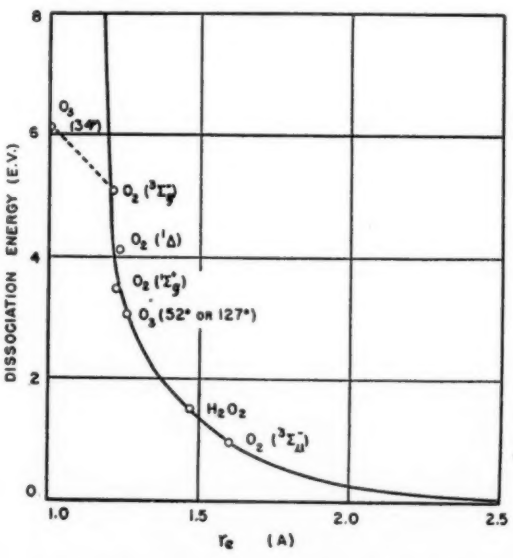

FIG. 1. Dissociation energy of oxygen-oxygen bonds *vs.* interatomic distance.

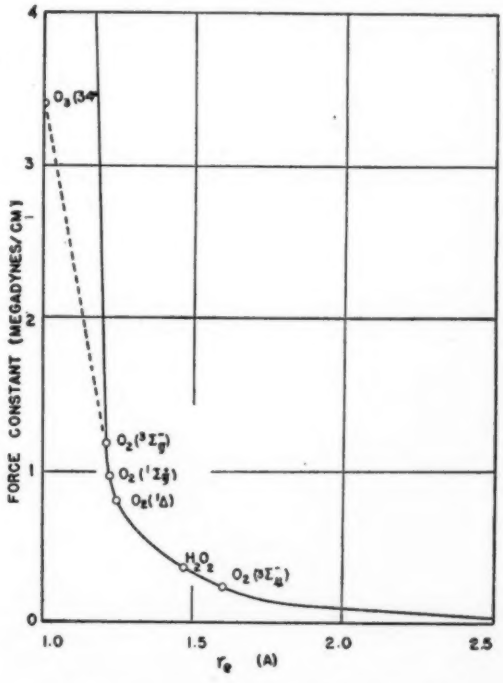

FIG. 2. Force constants of oxygen-oxygen bonds *vs.* interatomic distance.

atom attach themselves to the already existing oxygen bond, strengthening it, and decreasing its distance from 1.21A to 1.0A. It seems more reasonable to believe that the reverse happens. Even if it is assumed that all the binding energy (6.12 ev) resides in the 1A base bond, it can be seen from Fig. 1 that this situation does not fit into the energy-distance relation. Hence it is believed that the base line must be greater than 1.21A (oxygen molecule) and perhaps 1.26A. Therefore, for the 52° model, it is estimated from Fig. 2, that the constant c_2 is about 0.7 megadyne/cm and c_1 is about 0.38 megadyne/cm. It is realized that these considerations are based on the assumption that the bond energies and force constants of all O−O bonds are given by the relations shown in Figs. 1 and 2. The 52° model gives moments of inertia $I_A=51.1$ 10^{-40} g cm², $I_B=30.2\times10^{-40}$ g cm², and $I_C=20.9\times10^{-40}$ g cm², so that the quantity $2I_AI_B/(I_A+I_B)=38\times10^{-40}$ g cm². Adel and Dennison estimate $56\times10^{-40}\pm20$ percent.

[1] A. Adel and D. M. Dennison, J. Chem. Phys. **14**, 379 (1946).
[2] G. Hettner, R. Pohlman, and H. J. Schumacher, Zeits. f. Physik **91**, 372 (1934).